Received: 3 February 2025 | Revised: 3 June 2025 | Accepted: 16 June 2025

DOI: 10.1111/bph.70135

RESEARCH ARTICLE

Anti-nociceptive action of leonurine through TRPA1 and TRPV4 channels modulation

Matilde Marini[1] | Lorenzo Landini[1] | Elisabetta Coppi[2] | Martina Tesi[1] | Elisa Bellantoni[1] | Martina Chieca[1] | Emma Beatrice Croce[3] | Lorenzo Bonacchi[4] | Giulia Brancolini[1,5] | Piero Bruschi[6] | Daniel Souza Monteiro de Araújo[7] | Gaetano De Siena[1] | Alexandra Dimitrova[3] | Alessandra Mastricci[1] | Henrique Rocha Mendonça[8,9] | Irene Scuffi[1] | Martina Venturini[2] | Luiza Dos Santos Heringer[9] | Fabio Vaiano[3] | Romina Nassini[1] | Francesco De Logu[1]

[1]Department of Health Science, Clinical Pharmacology and Oncology Section, University of Florence, Florence, Italy

[2]Department of Neuroscience, Psychology, Drug Research and Child Health (NEUROFARBA), Section of Pharmacology and Toxicology, University of Florence, Florence, Italy

[3]Department of Health Science, Forensic Toxicology Laboratory FT-LAB, University of Florence, Florence, Italy

[4]Department of Information Engineering, University of Florence, Florence, Italy

[5]FloNext Srl, Florence, Italy

[6]Department of Agricultural, Environmental, Food and Forestry Science and Technology, University of Florence, Florence, Italy

[7]Graduate Program in Neurosciences, Neurobiology Department, Biology Institute, Fluminense Federal University, Niteroi, Brazil

[8]Integrated Lab of Morphology, Institute of Biodiversity and Sustainability NUPEM, Federal University of Rio de Janeiro, Macaé, Brazil

[9]Neurodegeneration and Repair Lab, Department of Pathology, Postgraduate Program in Anatomical Pathology, Faculty of Medicine, Federal University of Rio de Janeiro, Rio de Janeiro, Brazil

Correspondence
Romina Nassini and Francesco De Logu, Department of Health Sciences, Clinical Pharmacology and Oncology Section, University of Florence, Florence, 50139, Italy.
Email: romina.nassini@unifi.it; francesco.delogu@unifi.it

Funding information
#NEXTGENERATIONEU (NGEU); and the Ministry of University and Research (MUR), National Recovery and Resilience Plan (NRRP), project MNESYS (PE0000006) – A Multiscale integrated approach to the study of the nervous system in health and disease (DR. 1553 11.10.2022) (F.D.L.). Next Generation EU, National Recovery and

Background and Purpose: Leonurine, a pseudoalkaloid derived from *Leonotis leonurus*, has been traditionally used in herbal medicine to alleviate conditions such as headaches and abdominal discomfort. Its therapeutic effects are often attributed to potential antioxidant properties; however, the precise molecular mechanisms remain poorly understood. Transient Receptor Potential (TRP) channels, particularly **TRPA1** and **TRPV4**, serve as critical sensors of reactive oxygen species (ROS). Persistent ROS elevation can contribute to pain by activating these channels.

Experimental Approach: Here, we examined the antinociceptive properties of leonurine and its modulatory effects on TRPA1 and TRPV4 channels after stimulation with selective (allyl isothiocyanate (**AITC**) and **GSK1016790A**, respectively) or non-selective (hydrogen peroxide, **H_2O_2**) agonists. Employing human and murine cell lines

Abbreviations: AAV, adeno associated virus; Adv, Advillin; AITC, allyl-isothiocyanate; BL, Baseline; CIPN, chemotherapy-induced peripheral neuropathy; H_2O_2, hydrogen peroxide; ROS, reactive oxygen species; TRP, transient receptor potential; TRPA1, transient receptor potential Ankyrin 1; TRPV4, transient receptor potential Vanilloid 4.

Matilde Marini, Lorenzo Landini and Elisabetta Coppi have contributed equally to this work.

Romina Nassini and Francesco De Logu have contributed equally to this work.

Resilience Plan, Mission 4 Component 2 – Investment 1.4 – National Center for Gene Therapy and Drugs based on RNA Technology – CUP B13C22001010001 (R.N.).

expressing TRPA1 and TRPV4, and mouse primary sensory neurons from dorsal root ganglia (DRG), we observed that leonurine elicited a selective, concentration-dependent increase in intracellular calcium levels, followed by desensitisation of both channels. Notably, TRPA1 and TRPV4 have been implicated in the development and maintenance of mechanical allodynia within models of chemotherapy-induced peripheral neuropathy (CIPN). We used a **thalidomide** CIPN model to assess the efficacy of leonurine to reduce TRPA1- and TRPV4-dependent mechanical allodynia.

Key Results: Our findings indicate that repeated, but not acute, administration of leonurine significantly reduced thalidomide-induced mechanical allodynia, highlighting the crucial role of TRPA1 and TRPV4 desensitisation in pain modulation.

Conclusions and Implications: These results position leonurine as a promising candidate for pain management, warranting further investigation into long-term therapeutic strategies and potential clinical applications.

KEYWORDS
desensitisation, CIPN, leonurine, pain, ROS, TRPA1, TRPV4

1 | INTRODUCTION

Leonurine is a pseudoalkaloid compound, first isolated in 1930 from the *Leonotis leonurus* plant which has been traditionally used by South African communities for its medicinal properties. Extracts from *L. leonurus* exhibit a variety of biological activities, including anti-apoptotic, antioxidant, and anti-inflammatory effects (Huang et al., 2021; Liu et al., 2024). However, the natural content of leonurine in fresh *Leonurus* plants is relatively low (approximately 0.02%–0.12%), and coexisting phytochemicals introduce impurities. Consequently, large-scale generation of high-purity leonurine necessitates chemical synthesis (Zhu et al., 2018). Studies demonstrate protective effects of leonurine in multiple pathological conditions, including gynaecological, cardiovascular and central nervous system diseases (Huang et al., 2021; Lin et al., 2022; Xu et al., 2020). Many mechanisms have been proposed to explain these protective effects, some of which involve the inhibition of **nuclear factor kappa B** (NF-κB) activation and suppression of intracellular reactive oxygen species (ROS) production and accumulation (Huang et al., 2021; Zhang et al., 2012; Zhu et al., 2018). Notably, ROS contribute significantly to both the onset and persistence of pain, particularly in neuropathic pain models involving nerve injury (De Logu et al., 2017). Their involvement extends to conditions such as alcohol-induced peripheral neuropathy (De Logu et al., 2019), diabetic neuropathy (Cameron et al., 2001) and both tumour progression and chemotherapy-induced peripheral neuropathy (CIPN) (Boiko et al., 2017; De Logu et al., 2016, 2020; Materazzi et al., 2012; Nassini et al., 2012; Shim et al., 2019; Trevisan et al., 2013).

The **Transient Receptor Potential (TRP) channel superfamily** includes a subclass of non-selective, calcium ion (Ca^{2+})-permeable channels, predominantly expressed in a subset of sensory neurons (Nassini et al., 2012; Sousa-Valente et al., 2014). Among these, the ankyrin 1 (**TRPA1**) and vanilloid 4 (**TRPV4**) have gained attention because of their role in various physiological and pathological processes (Al-Anzi et al., 2006). TRPA1 is activated by exogenous compounds such as **allyl isothiocyanate** (mustard oil) and **cinnamaldehyde** (Jordt et al., 2004; Nilius & Voets, 2007), in contrast, TRPV4 is activated by different physical and chemical stimuli, including hypotonic

What is already known?

- Leonurine has traditional use for pain relief, possibly because of antioxidant properties.
- TRPA1 and TRPV4 channels mediate pain via reactive oxygen species in neuropathy.

What does this study add?

- Leonurine desensitises TRPA1 and TRPV4 channels after activating calcium influx in sensory neurons.
- Repeated leonurine treatment reduces thalidomide-induced mechanical and cold sensitivity in mice.

What is the clinical significance?

- Leonurine reduces pain via partial TRPA1/TRPV4 agonism and resulting neuronal desensitisation.
- Leonurine is a promising pain therapy targeting redox-sensitive ion channels in sensory neurons.

cell swelling (Liedtke et al., 2000), heat (Guler et al., 2002; Watanabe et al., 2002), low pH (Suzuki et al., 2003) and membrane stretch and shear stress (Liedtke & Friedman, 2003; Mendoza et al., 2010). Furthermore, both TRPA1 and TRPV4 channels are known to sense ROS, including **hydrogen peroxide** (H_2O_2) (Mori et al., 2016). This redox sensitivity is a distinctive feature, making TRPA1 and TRPV4 two of the major redox-sensitive channels within the TRP superfamily (Andersson et al., 2008; Jordt et al., 2004; Mori et al., 2016; Nilius & Voets, 2007).

Although decoctions and infusions of *L. leonurus* leaves are known to exhibit analgesic properties (Ojewole, 2005) and leonurine itself has been investigated as an effective remedy for several painful states, including postpartum abdominal pain (Kuchta et al., 2010), the precise molecular mechanism underlying leonurine-induced analgesia remains unknown.

Given the established roles of TRPA1 and TRPV4 in detecting ROS and the potential anti-inflammatory effects of leonurine through ROS modulation, here we investigated whether *L. leonurus* extracts could target TRPA1 and TRPV4 to provide pain relief. Our findings indicate that leonurine selectively targets both human and murine TRPA1 and TRPV4 channels, initially causing neuronal excitation followed by the desensitisation of both channels. We previously demonstrated that TRPA1 and TRPV4 channels mediate **thalidomide**-induced peripheral neuropathy in mice via a ROS-dependent pathway (De Logu et al., 2020). Here, we further explored the ability of leonurine to desensitise both TRPA1 and TRPV4 channels resulting in a reduction of mechanical allodynia in a mouse model of CIPN induced by thalidomide. Our findings suggest that the present and previously reported effect of *Leounurus* plants in pain sensation may derive from the ability of leonurine to evoke TRPA1 and TRPV4-dependent desensitisation of nociceptors, thereby reducing pain perception.

2 | METHODS

2.1 | Ethics

The conducted research complies with all relevant ethical regulations. Animal experiments were carried out in accordance with the European Union (EU) guidelines for animal care procedures and the Italian legislation (DLgs 26/2014) application of the EU Directive 2010/63/EU. The study was approved by the National Committee for the Protection of Animals used for Scientific Purposes of the Italian Ministry of Health (research permits #1194/2015PR). Animal studies are reported in compliance with the ARRIVE guidelines (Percie du Sert et al., 2020) and with the recommendations made by the *British Journal of Pharmacology* (Lilley et al., 2020).

2.2 | Cell lines

Human embryonic kidney cells (HEK293) were stably transfected with cDNA for human TRPA1 (hTRPA1-HEK293), or with cDNA for human TRPV4 (hTRPV4-HEK293) or with cDNA for human **TRPV1** (hTRPV1-HEK293). HEK293T cells (American Type Culture Collection ATCC® Cat#CRL-3216, RRID:CVCL_0063) and human breast adenocarcinoma MDA-MB-231 cells (ATCC® Cat#HTB-26™, RRID:CVCL_0062) were cultured in Dulbecco's Modified Eagle Medium (DMEM) supplemented with heat-inactivated foetal bovine serum (FBS) (10%) (FBS tetracycline free for hTRPV4-HEK293 cells), L-glutamine (2 mM), penicillin (100 U ml^{-1}), and streptomycin (10 mg ml^{-1}) at 37°C in 5% CO_2 and 95% O_2. The cell culture medium of hTRPA1–HEK293 cells also contained sodium pyruvate (1 mM) and G418 (1 mg ml^{-1}). Hygromycin B (100 μg ml^{-1}) and blasticidin S hydrochloride (5 μg ml^{-1}) and tetracycline (0.1 μg ml^{-1} overnight [ON] before Ca^{2+} imaging) were added to the hTRPV4–HEK293 cell culture medium. hTRPV1-HEK293 cells were selected with G418 (1 μl ml^{-1}). HEK293T cells were transiently transfected with the cDNAs (1 μg) coding for murine TRPA1 (Vector Builder, Chicago, Illinois, USA, #Trpa1 [NM_177781.5] Mouse Tagged ORF Clone, mTRPA1-HEK293T cells) or murine TRPV4 (OriGene, Rockville, MD 20850, US #Trpv4 [NM_022017] Mouse Tagged ORF Clone MG226813, mTRPV4-HEK293T cells) using the jetPRIME transfection reagent (Polyplus-transfection® SA, Strasbourg, France #101000006) 24 h before Ca^{2+} imaging experiments according to the manufacturer's protocol and cultured as described earlier. All cells were used when received without further authentication.

2.3 | Primary culture of mouse dorsal root ganglion (DRG) neurons

Primary DRG (combined cervical, thoracic, and lumbar) neurons were obtained from male C57BL/6J ($n = 10$), *Trpa1*$^{-/-}$ ($n = 5$) and *Trpv4*$^{-/-}$ ($n = 5$) adult mice. Briefly, tissues were bilaterally excised under a dissection microscope and enzymatically digested using 2 mg ml^{-1} of collagenase type 1A and 1 mg ml^{-1} of papain in Hanks' Balanced Salt Solution (HBSS) for 35 min at 37°C. Ganglia were then disrupted by several passages through a series of syringe needles (23–25 G). Neurons were then pelleted by centrifugation at 1200 rpm for 5 min at room temperature (RT) and resuspended in DMEM supplemented with Ham's-F12, containing 10% heat-inactivated FBS, 100 U ml^{-1} of penicillin, 0.1 mg ml^{-1} streptomycin, and 2 mM L-glutamine added with 100 ng ml^{-1} nerve growth factor and 2.5 mM cytosine-b-D-arabinofuranoside free base and maintained at 37°C in 5% CO_2 and 95% O_2 for 2 days before Ca^{2+}-imaging experiments.

2.4 | Calcium imaging

hTRPA1–HEK293, hTRPV4–HEK293, hTRPV1–HEK293, MDA-MB-231, mTRPA1-HEK293T, mTRPV4-HEK293T cells and mouse DRG neurons were plated on poly-L-lysine-coated (8.3 μM) 35-mm glass coverslips (Thermo Fisher Scientific, Waltham, MA) and maintained at 37°C in 5% CO_2 and 95% O_2 for 24 h before Ca^{2+} imaging. On the

day of experiments, cells were loaded (40 min) with Fura-2 AM-ester (5 μM) added to the buffer solution (37°C) containing (in mM) 2 $CaCl_2$, 5.4 KCl, 0.4 $MgSO_4$, 135 NaCl, 10 D-glucose, 10 4-(2-hydroxyethyl)-1-piperazineethanesulfonic acid and bovine serum albumin (BSA, 0.1%) at pH 7.4. Cells were then washed and transferred to a chamber on the stage of a fluorescent microscope for recording (Axio Observer 7; with a fast filter wheel and Digi-4 lens to record excitations and Ultra-fast Sutter Lambda DG4 Xenon excitation source (range 300–700 nM) (Zeiss, Oberkochen, Germany). Depending on the experiment, cells were exposed to leonurine (300 nM to 1 mM) or vehicle (0.1% DMS0), allyl isothiocyanate (AITC, 300 nM to 1 mM) or vehicle (0.1% DMS0), **capsaicin** (10 μM) or vehicle (0.1 ethanol), **GSK-1016790A** (3 nM to 300 μM) or vehicle (0.1% DMS0) and **hydrogen peroxide** (H_2O_2 300 μM to 20 mM) or vehicle (0.01% dimethyl sulfoxide [DMSO]). For the Ca^{2+} assay experiments in MDA-MB-231 cells, a concentration of leonurine (126 μM) was selected that fell between the EC_{80} values of leonurine in hTRPA1-HEK293 and hTRPV4-HEK293 cells. EC_{80} agonist concentration was used in the presence of **A967079** (30 μM), **HC067047** (50 μM), Ca^{2+} free medium, H_2O_2 or vehicle (0.01–0.1% DMSO).

In the experiments involving mouse DRG neurons, a high concentration of KCl (50 mM) that depolarises functional neurons causing Ca^{2+} influx was used to further exclude the non-neuronal cells. The percentage of DRG neurons in each acquisition field that did not respond to the TRPA1 agonist, the TRPV4 agonist or both was consistent with previously reported data (Cao et al., 2009; Girard et al., 2013; Jordt et al., 2004; Nagata et al., 2005) (42.7 ± 2.6% non-responders for TRPA1, 12.2 ± 1% non-responders for TRPV4, and 11.5 ± 4.6% non-responders for both TRPA1 and TRPV4). The average trace (coloured trace) and the standard error (grey area) were derived from the mean response of all recorded cells in an experiment, including neurons that did not respond to TRPA1, TRPV4 or both. EC_{50}, EC_{80} and Emax were indicated as percentage of the response evoked by **ionomycin** (5 μM). Results were expressed as the percent increase in ratio 340/380 ($R_{340/380}$) over baseline normalised to the maximum effect induced by ionomycin added at the end of each experiment.

2.5 | Quantitative reverse transcription polymerase chain reaction (qRT-PCR)

Total RNA was extracted from hTRPA1–HEK293, hTRPV4–HEK293, MDA-MB-231 cells and mouse DRGs (combined cervical, thoracic and lumbar) using the RNeasy Mini kit (Qiagen SpA, Hilden, Germany), according to the manufacturer's protocol. RNA concentration and purity were assessed spectrophotometrically by measuring the absorbance at 260 and 280 nm. RNA was reverse transcribed with the SuperScript™ IV VILO™ Master Mix (Invitrogen, Waltham, Massachusetts, USA) following the manufacturer's protocol. For mRNA relative quantification, rt-PCR was performed on Rotor Gene® Q (Qiagen SpA, Rotor-Gene® Q Software Version 2.3.1.49). The relative abundance of mRNA transcripts was calculated using the Δ^{CT} method and normalised to GAPDH levels. Primers sets are listed in Table S1. Each experiment was independently repeated three times, and each experiment included three biological replicates.

2.6 | Electrophysiology

Whole-cell patch-clamp recordings were performed in primary sensory neurons (C57BL/6J adult mice, $n = 10$ mice) plated on coated coverslips as previously reported (Benemei et al., 2017). Briefly, coverslips were transferred to a recording chamber (500 μl volume), mounted on the platform of an inverted microscope (Olympus CKX41, Milan, Italy) and superfused at a flow rate of 1.5 ml min^{-1} with a standard extracellular solution containing (in mM): 10 HEPES, 10 D-glucose, 147 NaCl, 4 KCl, 1 $MgCl_2$ and 2 $CaCl_2$ (pH adjusted to 7.4 with NaOH). Cells were voltage-clamped at −60 mV by a 2–4 MΩ-recording electrode filled with the following intracellular solution (in mM): CsCl 120; Mg_2-ATP 3; EGTA 10 and HEPES 10 (pH 7.4 with CsOH). All the experiments were performed at room temperature (RT: 20–22°C). Data were acquired by an Axopatch 200B amplifier (Axon Instruments, Union City, CA), low-pass filtered at 10 kHz, stored and analysed with pClamp 9.2 software (Axon Instruments). Series resistance (R_s), membrane resistance (R_m) and membrane capacitance (C_m) were routinely measured by fast hyperpolarising 10 mV voltage steps. Only cells showing a stable C_m and R_s (<20% variation) throughout the experiment were included in the analysis. TRPA1-, TRPV4- or TRPV1-mediated currents were detected as inward currents activated upon superfusion with respective agonists: AITC (200 μM) GSK-1016790A (10 μM) or capsaicin (10 μM), respectively. Averaged TRP-activated currents were normalised to C_m and expressed as current density (pA/pF) in averaged results.

2.7 | MTT cell viability assay

Cells were plated in 96-well black wall clear bottom plates (#165305, Thermo Fisher Scientific, Waltham, MA, USA) and maintained at 37°C in 5% CO_2 and 95% O_2 for 24 h before the experiments. Depending on the experiments, each cell line was incubated for 10 min with the highest concentration of different compounds tested in calcium imaging experiments. Specifically, leonurine (hTRPA1-HEK293 = 1 mM, hTRPV4-HEK293 = 1 mM, hTRPV1-HEK293 = 126 μM, HEK293T = 126 μM, MDA-MB-231 = 126 μM, mTRPA1-HEK293T = 1 mM, mTRPV4-HEK293T = 300 μM and mDRG neurons = 115 μM), AITC (hTRPA1-HEK293 = 1 mM, MDA-MB-231 = 300 μM, mTRPA1-HEK293T = 1 mM and mDRG neurons = 30 μM), GSK-1016790A (hTRPV4-HEK293 = 100 μM, MDA-MB-231 = 100 μM, mTRPV4-HEK293T = 300 μM and mDRG neurons = 1 μM), H_2O_2 (hTRPA1-HEK293 = 126 μM, hTRPV4-HEK293 = 5 mM, MDA-MB-231 = 20 mM, mTRPA1-HEK293T = 1 mM and mTRPV4-HEK293T = 300 μM), A967079 (30 μM),

HC067047 (50 μM), capsaicin (10 μM) and A967079 + HC067047 (30 μM + 50 μM), were tested. Vehicle (Hank's balanced salt solution, HBSS)-treated cells represented the maximum cell viability. Ionomycin (100 μM), as a positive control, was used to completely lyse the cells (Han et al., 2013). Then, the medium was removed and replaced with 50 μl of MTT diluted in HBSS (final concentration 0.5 mg ml^{-1}). Following a 4-h incubation period, DMSO was used to dissolve the formazan crystals, and the absorbance was measured at 570 nm after measuring the background absorbance of multiwell plates (690 nm) in a microplate reader (FlexStation 3 Multi-Mode microplate reader; Molecular Devices, San Jose, CA, USA) with SoftMax® Pro 7 software (Molecular Devices). The background absorbance was subtracted from the 570 nm measurement, and results were expressed as percentage of cell viability compared to vehicle.

2.8 | Animals

Male mice were used throughout (25–30 g, 6–8 weeks). In accordance with the 3R guidelines to minimise the number of animals and avoid possible confounding effects of hormone fluctuation in pain perception, only male mice were used (Kilkenny et al., 2010). The following mouse strain was used: C57BL/6J mice (Jackson Laboratories, Strain #000664, RRID:IMSR_JAX:000664) and hemizygous Advillin-Cre mice (Adv-Cre) (Zurborg et al., 2011). Hemizygous Advillin-Cre mice (*Adv-Cre*$^{+}$) or their control (*Adv-Cre*$^{-}$) were used for the infection with adeno associated virus (AAV) for selective silencing of *trpa1* or *trpv4* genes in primary sensory neurons.

For isolation of primary DRG neurons, TRPA1-deficient (Jackson Laboratories, Strain #:006401 *Trpa1*$^{-/-}$; B6129P-Trpa1$^{tm1Kykw/J}$; RRID:IMSR_JAX:006401) and TRPV4-deficient (*Trpv4*$^{-/-}$) (Liedtke & Friedman, 2003) mice (male 25–30 g, 6–8 weeks), generated by heterozygous mice on a C57BL/6J background, were used. The group size of $n = 8$ animals for behavioural experiments was determined by sample size estimation using G*Power [v3.1;(Faul et al., 2007)] to detect size effect in a post hoc test with type 1 and 2 error rates of 5 and 20%, respectively. Mice were allocated to vehicle or treatment groups using a randomisation procedure (http://www.randomizer.org/). The assessors were blinded to the identity of the animals (allocation to treatment groups). None of the animals were excluded from the study. Behavioural studies followed the Animal Research: Reporting of In Vivo Experiments (ARRIVE) guidelines (McGrath & Lilley, 2015) (Kilkenny et al., 2010). Animals were euthanised with inhaled CO_2 plus 10–50% O_2. Mice were housed in a temperature (20 ± 2°C) and humidity (50 ± 10%) controlled *vivarium* (12 h dark/light cycle, free access to food and water, five animals per cage). At least 1 h before behavioural experiments, mice were acclimatised to the experimental room and behaviour was evaluated between 9:00 AM and 5:00 PM. All the procedures were conducted following the current guidelines for laboratory animal care and the ethical guidelines for investigations of experimental pain in conscious animals set by the International Association for the Study of Pain (Zimmermann, 1983).

2.8.1 | Treatment protocols

C57BL/6J mice received single or repeated (seven consecutive days) local (intraplantar, i.pl. 10 μl) administration (10 and 40 nmol) of leonurine or Veh (4% DMSO and 4% Tween 80 in 0.9% NaCl) before the algogenic stimulus, represented by AITC (10 nmol per 10 μl, i.pl.) or GSK-1016790A (2.5 nmol per 10 μl, i.pl.) or Veh (1% DMSO in 0.9% NaCl). In other experimental sets, mice received a single injection (intraperitoneal, i.p. 10 ml kg^{-1}) of thalidomide (50 mg kg^{-1}) or vehicle (4% DMSO, and 4% Tween 80 in 0.9% NaCl). After that, mice received single or repeated (seven consecutive days) i.pl. or intrathecal (i.th., 5 μl) administration of leonurine (10 nmol). The i.pl. administration ensures localised drug delivery, specifically targeting peripheral nociceptive pathways. Conversely, the i.th. administration is employed to assess central modulation of pain, potentially affecting spinal processing of nociceptive signals. A single dose administered before the stimulus allows for the evaluation of acute analgesic effects, while repeated dosing enables the assessment of potential receptor desensitisation. No significant toxicity has been reported (Liu et al., 2024; Ojewole, 2005). *Adv-Cre*$^{+}$ and control mice were infected with an intravenous (i.v. 5 μl, 1×10^{12} v g^{-1}) injection of different AAVs 3 weeks before thalidomide injection.

2.9 | Plasmids construction

pAAV[FLEXon]-CMV LL-rev (EGFP-5′ miR-30E-BfuAI ORF_44bp BfuAI-3′ miR-30E)-rev (LL)-WPRE was used as backbone to express short hairpin RNAs targeting the gene of interest. mTrpa1shRNA (primers P1/P2) and mTrpv4 shRNA (P3/P4) were cloned by replacing the 44 bp ORF with pre-annealed and phosphorylated oligonucleotides (T4 PNK (NEB, #M0201S) by using BfuAI compatible bases. Plasmid constructs were confirmed by Sanger sequencing. Primer sequences are reported in Table S1.

2.10 | AAV generation

AAVpro293T cells (#632273, Takara) were maintained in DMEM high glucose with 10% heat inactivated FBS, 1 mM penicillin/streptomycin, 4 mM L-glutamine and 1 mM sodium pyruvate at 37°C in 5% CO_2 and 95% O_2.

2.10.1 | AAV production and cell lysis

Three days before transfection, AAVpro cells were seeded in a CellBIND Polystyrene CellSTACK 2 Chamber (#3310, Corning, Corning, NY, USA) for 48 h to reach 80% confluence. The day before transfection, 250 million cells were seeded in a CellBIND Polystyrene CellSTACK 5 Chamber (#3311; Corning) for 24 h, until 80% of confluence. AAVpro 293T cells were then triple transfected with polyethylenimine (#23966, PEI, Polyscience) using a DNA:PEI ratio of 1:3.

Transfection was performed with 2.5 mg total DNA with 1:1:1 M ratio of three plasmids (plasmid expressing mTRPV4 shRNA [5′-ACCTGGAGACAGTTCTCAACAA-3′] or mTRPA1 shRNA [5′-AGCTAAGCTGTGTAAATCAAAT-3′], pAdDeltaF6 [#11287, Addgene] and Rep/Cap). To infect with high efficiency primary sensor neurons, Rep/Cap2/B10 was used (pAAV AAV2 rep-AAV.CAP-B10 #175004, Addgene). After 72 h, AAV virions were collected. Cells were harvested and transferred into 50 ml conical tubes and centrifuged at 1200 × *g* for 10 min at 4°C. The supernatant was filtered through 0.45 μm polyethersulfone (PES) membranes, and then 25 ml of 40% PEG solution pH 7.4 (400 g of PEG 8000 + 24 g of NaCl in ddH_2O to a final volume of 1.000 ml) was added to every 100 ml of filtered supernatant. The solution was slowly stirred at 4°C for 1 h and then kept for 3 h without stirring at 4°C to allow full precipitation of AAV particles. After centrifugation at 2900 × *g* for 15 min at 4°C, supernatant was discarded and pellet containing virion particles was resuspended in a10 ml of PBS/pluronic F68 (0.001%)/NaCl (200 mM) solution. The AAVpro cell pellet, derived from first centrifugation, was directly resuspended in 10 ml of PBS/Pluronic F68 (0.001%)/NaCl (200 mM) solution and lysed by 4 cycles of freezing at −80°C for 30 min, followed by a thaw at 37°C for 10 min. After centrifugation at 3.200 × *g* for 15 min at 4°C, supernatant containing the AAV particles was collected. Both samples obtained from supernatant and cell pellet were mixed, incubated with Benzonase (50 U ml^{-1}) at 37°C for 45 min to remove residual DNA carried over AAV packaging process. Then, sample was centrifuged at 2.500 × *g* for 10 min at 4°C, and clarified supernatant was transferred to new tube and it was kept overnight at 4°C before iodixanol purification.

2.10.2 | AAV purification by iodixanol gradient

A gradient of iodixanol was prepared. Starting with a 60% iodixanol solution (OptiPrep; STEMCELL Technologies, Vancouver, Canada), a 15% iodixanol solution (4.5 ml of iodixanol [60%] + 13.5 ml of NaCl/PBS-MK buffer [1 M]), a 25% solution (5 ml of iodixanol [60%] + 7 ml of PBS-MK buffer [1×] + 30 μl of Phenol red), a 40% solution (6.7 ml of iodixanol [60%] + 3.3 ml of PBS-MK buffer [1×]) and a 60% solution (10 ml of iodixanol [60%] + 45 μl of Phenol red) were made. Each solution was added into a 39-ml Quick-Seal tube (Beckman Coulter, Brea, CA, USA) using an 18 G needle syringe in the following order: 8 ml of 15% of iodixanol solution, 6 ml of 25% iodixanol solution, 5 ml of 40% iodixanol solution and 5 ml of 60% iodixanol solution. Finally, Quick-Seals were filled with the AAV solution on the top, sealed and ultracentrifuged in a Type 70 Ti rotor (Beckman Coulter) at 350.000 × *g* at 10°C for 1.5 h. Then, Quick-Seal tubes were pierced with a 16 G needle on top and a 14 G needle at the interface between the 60% and 40% iodixanol gradients. Viral particles contained in the 40% iodixanol layer were collected drop by drop in 2-ml microcentrifuge tubes, combined and concentrated using Amicon Ultra-15 centrifugal filter units (molecular weight cut-off, 100 kDa; Merck Millipore). Before the concentration step, Amicon membranes were covered with 15 ml of 0.1% Pluronic F68/PBS solution for 10 min, discarded and replaced with 15 ml of 0.01% Pluronic F68 in PBS solution. Tubes were centrifuged at 3.000 rpm for 5 min at 4°C, and the flowthrough was discarded. Around 15 ml of 0.001% Pluronic F68 in PBS + NaCl 200 mM solution was added and centrifuged at 3.000 × rpm for 5 min at 4°C, and the flowthrough was again discarded. During the concentration process, a buffer exchanged was made with formulation buffer (FB, 0.001% Pluronic F68 in PBS). FB was added to the AAV-iodixanol sample to replace iodixanol and to avoid toxicity in animals after AAV injection. rAAV were aliquoted and stored at −80°C. The viral titre was quantified using RT-qPCR.

2.11 | Behavioural experiments

2.11.1 | Acute nociception

Immediately after i.pl. injection, mice were placed inside a plexiglass chamber, and spontaneous nociception was assessed for 10 min by measuring the time (seconds) that the animal spent licking/lifting the injected paw.

2.11.2 | Hindpaw mechanical allodynia

The mechanical paw-withdrawal threshold was measured using von Frey filaments of increasing stiffness (0.02–2 g) applied to the plantar surface of the mouse hind paw, according to the up-and-down paradigm (Chaplan et al., 1994). The 50% mechanical paw-withdrawal threshold (g) response was then calculated from the resulting scores.

2.11.3 | Cold response

Cold sensitivity was assessed by measuring the acute nociceptive response to acetone-evoked evaporative cooling. Briefly, mice were placed in a wire mesh floor cage and, after habituation, a droplet (20 μl) of acetone, formed on the flat-tip needle of a syringe, was gently touched to the plantar surface of the hind paw, and the time spent in elevation and licking of the plantar region over a 60-s period was measured. Acetone was applied three times at 10- to 15-min intervals and the average elevation/licking time was calculated.

2.12 | Materials

Allyl isothiocyanate (#377430), capsaicin (#M2028), GSK1016790A (#G0798), thalidomide (#T144) and all other reagents, unless otherwise specified, were from Merck Life Science S.r.l. (Milan, Italy). Leonurine was from DBA (#HY-N0741, Milan, Italy) with a purity of 99.64%. Details of other materials from different suppliers are provided in the relevant sections.

2.13 | Data and statistical analysis

The data and statistical analysis comply with the recommendations of the *British Journal of Pharmacology* on experimental design and analysis in pharmacology (Curtis et al., 2018). The results are expressed as the mean ± SEM. Before statistical significance analysis was performed, data were tested for normality using the Kolmogorov–Smirnov test and for homogeneity using the Bartlett test. Statistical analysis was undertaken only where the size of each group was at least $n = 5$. The reported group/sample size is the number of independent values, and that statistical analysis was performed using these independent values (i.e. not treating technical replicates as independent values). For multiple comparisons, a one-way analysis of variance (ANOVA) followed by a post hoc Bonferroni's test was used. The two groups were compared using Student's *t*-test. For behavioural experiments with repeated measures, a two-way mixed-model ANOVA followed by a post hoc Bonferroni's test was used. Statistical analyses were performed on raw data using GraphPad Prism 8 (GraphPad Software Inc.). *P*-values less than 0.05 ($P < .05$) were considered significant. *P*-values under 0.05, 0.01, 0.001 and 0.0001 are indicated with one, two, three and four asterisks, paragraph or hashtag symbols, respectively. EC_{50} values were determined from nonlinear regression models using GraphPad Prism 8. The statistical tests used and group/sample size for each analysis are shown in the figure legends.

2.14 | Nomenclature of targets and ligands

Key protein targets and ligands in this article are hyperlinked to corresponding entries in https://www.guidetopharmacology.org, and are permanently archived in the Concise Guide to PHARMACOLOGY 2023/2024 (Alexander et al., 2023).

3 | RESULTS

3.1 | Leonurine targets human and murine TRPA1 and TRPV4 channels

In both human TRPA1 and TRPV4-HEK293T transfected cells (hTRPA1-HEK293 and hTRPV4-HEK293), leonurine elicited a concentration-dependent calcium (Ca^{2+}) increase (hTRPA1: $EC_{50} = 26$ μM [CI: 20–35 μM], $EC_{80} = 105$ μM [CI: 80–139 μM]; hTRPV4: EC_{50} 37 μM [CI: 31–43 μM], EC_{80} 146 μM [CI: 124–173 μM], respectively) that was absent in the presence of the selective antagonists (A967079 [A96] 30 μM and HC067047 [HC06] 50 μM, respectively) and in a Ca^{2+}-free medium (Figure 1a,b and Table 1). The efficacy of leonurine was significantly lower ($P < 0.0001$) compared to AITC in hTRPA1-HEK293 cells (Emax leonurine = 55% [CI: ±1] and Emax AITC = 90% [CI: ±1]) and to GSK1016790A (GSK) ($P < 0.0001$) in hTRPV4-HEK293 cells (Emax leonurine = 55% [CI: ±1] and Emax GSK = 85% [CI: ±1]) (Figure 1a,b and Table 1). These results suggest that leonurine, a herbal-derived molecule, may act as a partial agonist. Leonurine (120 μM) did not evoke any response in hTRPV1-HEK293 cells, which were activated by capsaicin (CPS, 10 μM), and in untransfected HEK293T cells (Figure S1a, b). To assess the effect of leonurine in non-transfected cells that constitutively express the human TRPA1 and TRPV4 channels, we employed the human breast adenocarcinoma (MDA-MB-231) cell line. We confirmed the expression of the native human TRPA1 and TRPV4 mRNA as previously reported (Bera et al., 2022; Sanchez et al., 2024) and their functionality (Figures S1c and 1c). Then, we found that leonurine (126 μM) induced a Ca^{2+} response that was partially reduced by A96 and HC06 and totally abolished by the combination of the two antagonists (Figure 1d).

To test the activity of leonurine in the mouse homologue TRPA1 and TRPV4 (mTRPA1 and mTRPV4) channels, mTRPA1-HEK293T and mTRPV4-HEK293T cells were used. Cells stimulation with leonurine evoked a Ca^{2+} response significantly lower compared to the selective channel agonists ($P < 0.0001$) (mTRPA1-HEK293T: $EC_{50} = 21$ μM [CI: 17–26 μM], $EC_{80} = 83$ μM [CI: 68–103 μM], Emax leonurine = 55% [CI: ±1] and Emax AITC = 74% [CI: ±2]; mTRPV4-HEK293T: $EC_{50} = 8$ μM [CI: 6–12 μM], $EC_{80} = 32$ μM [CI: 21–46 μM], Emax leonurine = 38% [CI:±1] and Emax GSK = 78% [CI: ±1]). All the responses were attenuated by A96 and HC06, respectively (Figure 2a, b and Table 1). Leonurine did not evoke any Ca^{2+} response in Ca^{2+}-free medium (Figure 2a,b). The MTT assay was used to evaluate the cytotoxicity of all compounds used in the in vitro experiments. Treatment of all previous cell lines with the highest concentration of the compounds did not significantly reduce cell viability compared to the vehicle (Figure S1d–j).

3.2 | Leonurine activates and desensitise TRPA1 and TRPV4 channels in murine nociceptors

Exposure of cultured primary sensory neurons derived from C57BL/6J mouse dorsal root ganglia (mDRG) to leonurine resulted in a concentration-dependent increase in the Ca^{2+} response ($EC_{50} = 29$ μM [CI: 23–37 μM] $EC_{80} = 115$ μM [CI: 91–148 μM]) (Figure 3a). The antagonists A96 and HC06 effectively blocked the Ca^{2+} increase induced by AITC (30 μM) and GSK (100 μM), respectively. However, when applied individually, they only partially reduced the leonurine-induced Ca^{2+} response (Figure 3a). Notably, the combined application of both A96 and HC06 completely abolished the leonurine-evoked Ca^{2+} response (Figures 3a and S2a).

To confirm the dual action of leonurine on TRPA1 and TRPV4 channels, DRG neurons were isolated from TRPA1 and TRPV4 knockout (*Trpa1*$^{-/-}$ and *Trpv4*$^{-/-}$, respectively) mice, where the selective TRPA1 and TRPV4 agonists failed to elicit any Ca^{2+} response (Figure S2b,c). Furthermore, leonurine-induced Ca^{2+} responses were significantly reduced in *Trpa1*$^{-/-}$ and *Trpv4*$^{-/-}$ compared to wild-type DRG neurons (Figure 3b,c). Additionally, the pretreatment of *Trpa1*$^{-/-}$ neurons with HC06 and *Trpv4* $^{-/-}$ neurons with A96 totally prevented the leonurine-dependent Ca^{2+}responses (Figure 3b,c).

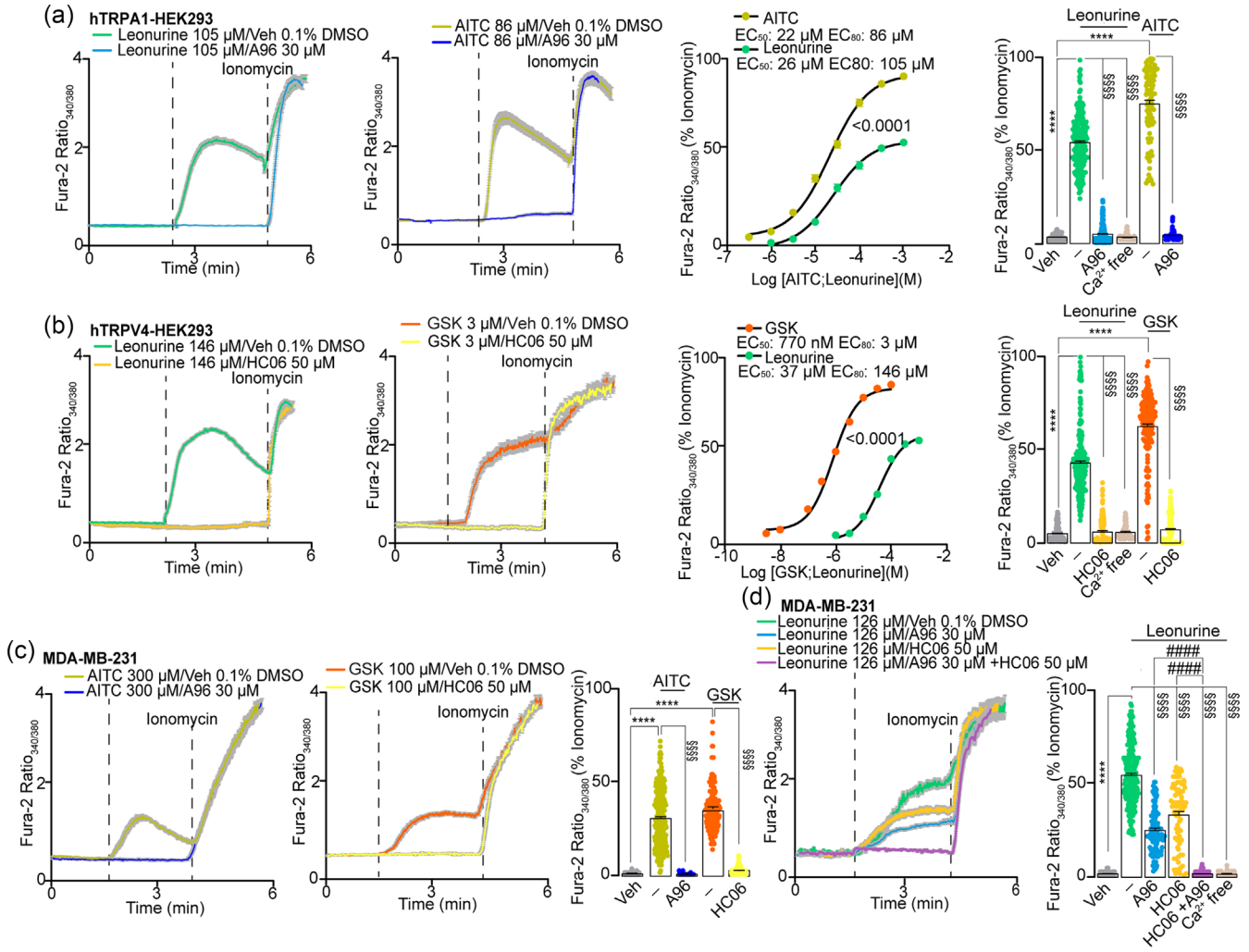

FIGURE 1 **Leonurine activates the human TRPA1 and TRPV4 channels.** (a) Typical traces, concentration-response curve (CRC) and pooled data of Ca^{2+} responses evoked by leonurine (CRC cells number: 1 μM $n = 125$, 3 μM $n = 117$, 10 μM $n = 77$, 30 μM $n = 291$, 100 μM $n = 166$, 300 μM $n = 101$, 1 mM $n = 101$; $n = 3$ independent experiments) and allyl isothiocyanate (AITC, CRC cells number: 300 nM $n = 110$, 1 μM $n = 235$, 3 μM $n = 191$,10 μM $n = 137$, 30 μM $n = 238$, 100 μM $n = 231$, 300 μM $n = 230$, 1 mM $n = 135$; $n = 3$ independent experiments) in hTRPA1-HEK293 cells, in the presence of vehicle (Veh, 0.001% DMSO), A967079 (A96) or Ca^{2+}-free medium (cells number: leonurine/Veh $n = 222$, leonurine/A96 $n = 100$, AITC/Veh $n = 100$, AITC/A96 $n = 100$, Ca^{2+}-free $n = 67$, Veh $n = 213$; $n = 3$ independent experiments). (b) Typical traces, CRC and pooled data of Ca^{2+} responses in hTRPV4-HEK293 cells stimulated with leonurine (CRC cells number: 1 μM $n = 96$, 3 μM $n = 350$, 10 μM $n = 276$, 30 μM $n = 171$, 100 μM $n = 114$, 300 μM $n = 65$, 1 mM $n = 112$; $n = 3$ independent experiments), and GSK1016790A (GSK, CRC cells number: 3 nM $n = 135$, 10 nM $n = 115$, 100 nM $n = 69$, 300 nM $n = 120$, 1 μM $n = 169$, 3 μM $n = 175$, 10 μM $n = 136$, 30 μM $n = 105$, 100 μM $n = 70$; n = 3 independent experiments), in the presence of Veh, HC067047 (HC06) or Ca^{2+}-free medium (cells number: leonurine/Veh = 240, leonurine/HC06 = 189, GSK/Veh = 175, GSK/HC06 = 147 Ca^{2+}-free $n = 64$, Veh $n = 133$; $n = 3$ independent experiments). (c) Typical traces and pooled data of Ca^{2+} responses in MDA-MB231 cells stimulated with AITC and GSK in the presence of Veh, A96 or HC06 (cells number: AITC/Veh $n = 246$, AITC/A96 $n = 70$, GSK/Veh $n = 156$, GSK/HC06 $n = 144$, Veh $n = 101$; $n = 3$ independent experiments). (d) Typical traces and pooled data of Ca^{2+}responses in MDA-MB-231 cells stimulated with leonurine, in the presence Veh A96, HC06, A96 + HC06 or Ca^{2+}-free medium (cells number: leonurine/Veh $n = 224$, leonurine/A96 $n = 107$, leonurine/HC06 $n = 84$, leonurine/A96 + HC06 $n = 118$, Ca^{2+}-free $n = 110$, Veh $n = 70$; $n = 3$ independent experiments). In typical trace graphs, the coloured line is the average calcium trace for all cells in a slide, in grey the SEM. Typical traces from different experiments are superimposed to qualitatively show the differences between treatments. The concentration of compounds in the cumulative data graph corresponds to those indicated in the typical traces. Dash (–) is a combination of vehicles. Data are mean ± SEM, one-way ANOVA, Bonferroni correction. $^{****}P < 0.0001$; $^{§§§§}P < 0.0001$; $^{####}P < 0.0001$.

It is known that ligand-gated ion channel receptors exhibit desensitisation after prolonged presence of an agonist (Benemei et al., 2017; Materazzi et al., 2013). Here we hypothesised that, acting as a partial agonist, leonurine could induce desensitisation of TRPA1 and TRPV4 channels, thereby attenuating their subsequent responses to selective agonists. To test this possibility, we developed desensitisation protocols using patch-clamp recordings of whole-cell membrane currents activated by selective TRPA1 or TRPV4 agonists,

TABLE 1 Half-maximal effective concentration (EC_{50}) and 80% maximal effective concentration (EC_{80}) and maximum effect (Emax) of leonurine, allyl isothiocyanate (AITC) and GSK1016790A (GSK) in cultured cells.

	Leonurine			AITC			GSK		
Cell type	EC_{50} (CI)	EC_{80} (CI)	E_{max}[a]	EC_{50} (CI)	EC_{80} (CI)	Emax[a]	EC_{50} (CI)	EC_{80} (CI)	E_{max}[a]
hTRPA1-HEK293	26 μM (20–35)	105 μM (80–139)	55% ± 1	22 μM (18–25)	86 μM (73–102)	90% ± 1	-	-	-
hTRPV4-HEK293	37 μM (31–43)	146 μM (124–173)	55% ± 1	-	-	-	770 nM (663–894)	3 μM (3–4)	85% ± 1
mTRPA1-HEK293T	21 μM (17–26)	83 μM (68–103)	55% ± 1	15 μM (12–18)	58 μM (46–73)	74% ± 2	-	-	-
mTRPV4-HEK293T	8 μM (6–12)	32 μM (21–46)	38% ± 1	-	-	-	6 μM 5–6)	23 μM (21–26)	78% ± 1

[a]Maximum effect expressed as percent of ionomycin.

applied either under control conditions or following leonurine exposure.

In cultured mDRG neurons, currents evoked by AITC (200 μM) or GSK (10 μM) were markedly desensitised after pre-exposure to leonurine (100 μM), confirming the role of leonurine in TRPA1 and TRPV4 excitation and desensitisation of mouse nociceptors (Figure 4a). Notably, capsaicin (10 μM)-evoked currents were not altered by previous application of leonurine (Figure 4a) (73.8 + −44.4 pA/pF in Veh vs 52.9 + −25.4 pA/pF after leonurine exposure in the AITC group and 62.5 + −27.8 pA/pF in Veh vs 59.4 + −27.8 pA/pF after leonurine exposure in the GSK group). Because the TRPV4 channel is only expressed in 54% of primary sensory neurons that express the TRPA1 channel (Kim et al., 2016), desensitisation was assessed separately for each channel. This approach complied with the 3Rs principles (Kilkenny et al., 2010), minimising the number of animals needed for DRG neurons isolation. Two consecutive AITC (200 μM) applications, separated by vehicle exposure, elicited similar currents (Figure 4b). However, when leonurine (100 μM) was applied in place of vehicle alone, the current evoked by the second AITC application was significantly reduced (Figure 4b). Similar results were obtained with GSK (10 μM) (Figure 4c). However, because desensitisation was observed for each channel independently, it can be hypothesised that in neurons co-expressing TRPA1 and TRPV4, desensitisation likely occurs in both channels. In line with this assumption, cells responding to both selective agonists applied consecutively presented both responses significantly reduced (Figure 4d) by previous leonurine (100 μM) application. The MTT assay confirmed that the treatment with the highest compound concentration did not result in a significant reduction in cell viability compared with vehicle in mouse DRG neurons (Figure S2d).

3.3 | Leonurine reduces H_2O_2-mediated TRPA1 and TRPV4 channels activation

We recently observed that ROS play a pivotal role in various murine models of chronic pain through the activation of neuronal and non-neuronal TRPA1 and TRPV4 channels, including cancer (De Logu et al., 2021; Landini, Marini, et al., 2023), migraine (De Logu et al., 2022; Landini, Monteiro, et al., 2023), endometriotic (Titiz et al., 2024) and neuropathic pain induced by either peripheral nerve injury (De Logu et al., 2019) or chemotherapeutic agents (Bellantoni et al., 2024; De Logu et al., 2020). We recently observed in a thalidomide mouse model of CIPN that, H_2O_2, a biomarker of oxidative stress, activates the TRPA1 (Andersson et al., 2008; Landini et al., 2022; Sawada et al., 2008) and the TRPV4 channels to induce the development and maintenance of chronic pain (De Logu et al., 2020). Here we tested the ability of leonurine to modulate the Ca^{2+} response induced by H_2O_2 in hTRPA1-HEK293 and mTRPA1-HEK293T, and hTRPV4-HEK293 and mTRPV4-HEK293T and MDA-MB-231 cells. We found that in the presence of leonurine, the H_2O_2-dependent Ca^{2+} responses were significantly reduced (Figure 5a–d). In addition, in MDA-MB-231 cells, A96 and HC06 only

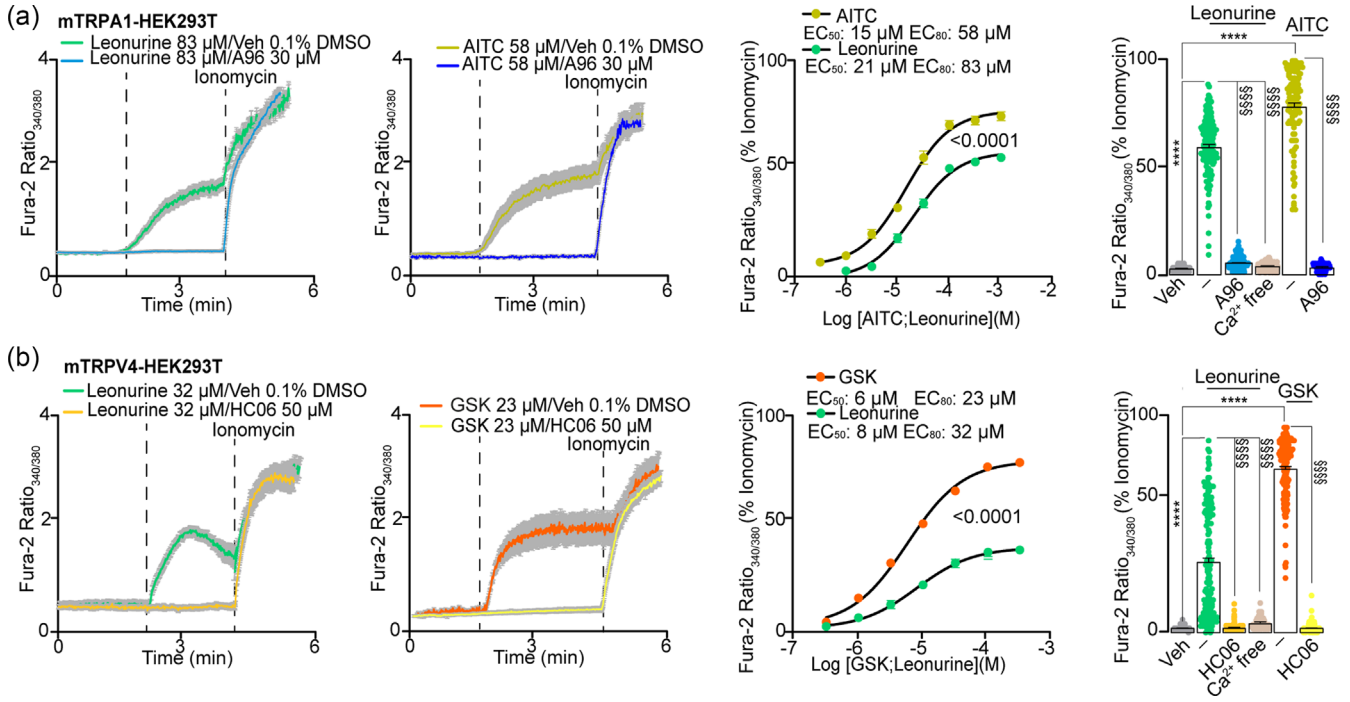

FIGURE 2 **Leonurine activates the murine TRPA1 and TRPV4 channels.** (a) Typical traces, CRC, and pooled data of Ca^{2+} responses in mTRPA1-HEK293T cells stimulated with leonurine (CRC cells number: 1 μM $n = 105$, 3 μM $n = 45$, 10 μM $n = 60$, 30 μM $n = 90$, 100 μM $n = 82$, 300 μM $n = 83$, 1 mM $n = 29$) and allyl isothiocyanate (AITC, CRC cells number: 300 nM $n = 71$, 1 μM $n = 71$, 3 μM $n = 79$, 10 μM $n = 118$, 30 μM $n = 122$, 100 μM $n = 112$, 300 μM $n = 85$, 1 mM $n = 85$) in the presence of vehicle (Veh) A967079 (A96) or Ca^{2+}-free medium (cells number: leonurine/Veh $n = 136$, leonurine/A96 $n = 131$, AITC/Veh $n = 112$, AITC/A96 $n = 57$, Ca^{2+}-free $n = 103$, Veh $n = 135$; $n = 3$ independent experiments). (b) Typical traces, CRC and pooled data of Ca^{2+} responses in mTRPV4-HEK293T cells stimulated with leonurine (CRC cells number: 300 nM $n = 104$, 1 μM $n = 61$, 3 μM $n = 52$, 10 μM $n = 124$, 30 μM $n = 158$, 100 μM $n = 41$, 300 μM $n = 148$) or GSK1016790A (GSK, CRC cells number: 300 nM $n = 71$, 1 μM $n = 78$, 3 μM $n = 85$, 10 μM $n = 114$, 30 μM $n = 72$, 100 μM $n = 109$, 300 μM $n = 68$) in the presence of Veh, HC067047 (HC06) or Ca^{2+}-free medium (cells number: leonurine/Veh $n = 156$, leonurine/HC06 $n = 109$, GSK/Veh $n = 126$, GSK/HC06 $n = 149$, Ca^{2+}-free $n = 75$, Veh $= 64$; $n = 3$ independent experiments). In typical trace graphs, the coloured line is the average calcium trace for all cells in a slide, in grey the SEM. Typical traces from different experiments are superimposed to qualitatively show the differences between treatments. The concentration of compounds in the cumulative data graph corresponds to those indicated in the typical traces. Dash (–) is a combination of vehicles. Data are mean ± SEM, one-way ANOVA, Bonferroni correction. **** $P < 0.0001$; §§§§ $P < 0.0001$; #### $P < 0.0001$.

partially attenuated the Ca^{2+} response evoked by H_2O_2 (20 mM). By contrast, leonurine (120 μM), similar to the combination of the two antagonists, completely abolished the response (Figure 5e). This further confirms leonurine's dual action on both TRPA1 and TRPV4 channels. The MTT assay confirmed that the treatment with H_2O_2 concentration did not result in a significant reduction in cell viability compared with vehicle for all cell lines (Figure S2e–i).

3.4 | Leonurine attenuates pain-like responses via TRPA1 and TRPV4 channels

A single intraplantar (i.pl. 10 μl) administration of leonurine (10 and 40 nmol) did not produce any significant acute nociceptive response or mechanical allodynia in C57BL/6J mice (Figure 6a). Furthermore, a single dose of leonurine (10 nmol, i.pl.) did not affect either the acute nociceptive response or mechanical allodynia evoked by AITC (10 nmol, i.pl.) or GSK (2.5 nmol, i.pl.) (Figure 6b,c). However, repeated administration of leonurine (10 nmol, i.pl.) for seven consecutive days before the application of the stimulus attenuated the acute nociceptive response and mechanical allodynia to AITC and GSK (Figure 6d,e). These findings suggest that prolonged leonurine treatment induces desensitisation of nociceptive behaviour and prolonged mechanical allodynia, specifically triggered by activators of the TRPA1 and TRPV4 channels.

To further investigate the dual role of leonurine in targeting TRPA1 and TRPV4 channels, we replicated a model of CIPN induced by thalidomide. In this model, we have previously shown that both TRPA1 and TRPV4 channels cooperate to the development and maintenance of mechanical allodynia, and TRPA1 is implicated in the development of cold allodynia (De Logu et al., 2020). Our previous findings indicated that in the thalidomide-induced CIPN mouse model, the involvement of TRPA1 and TRPV4 channels was associated with thalidomide-induced ROS production. Notably, their contributions were spatially and anatomically distinct, with TRPA1 playing a peripheral role, whereas TRPV4 contributed centrally (De Logu et al., 2020).

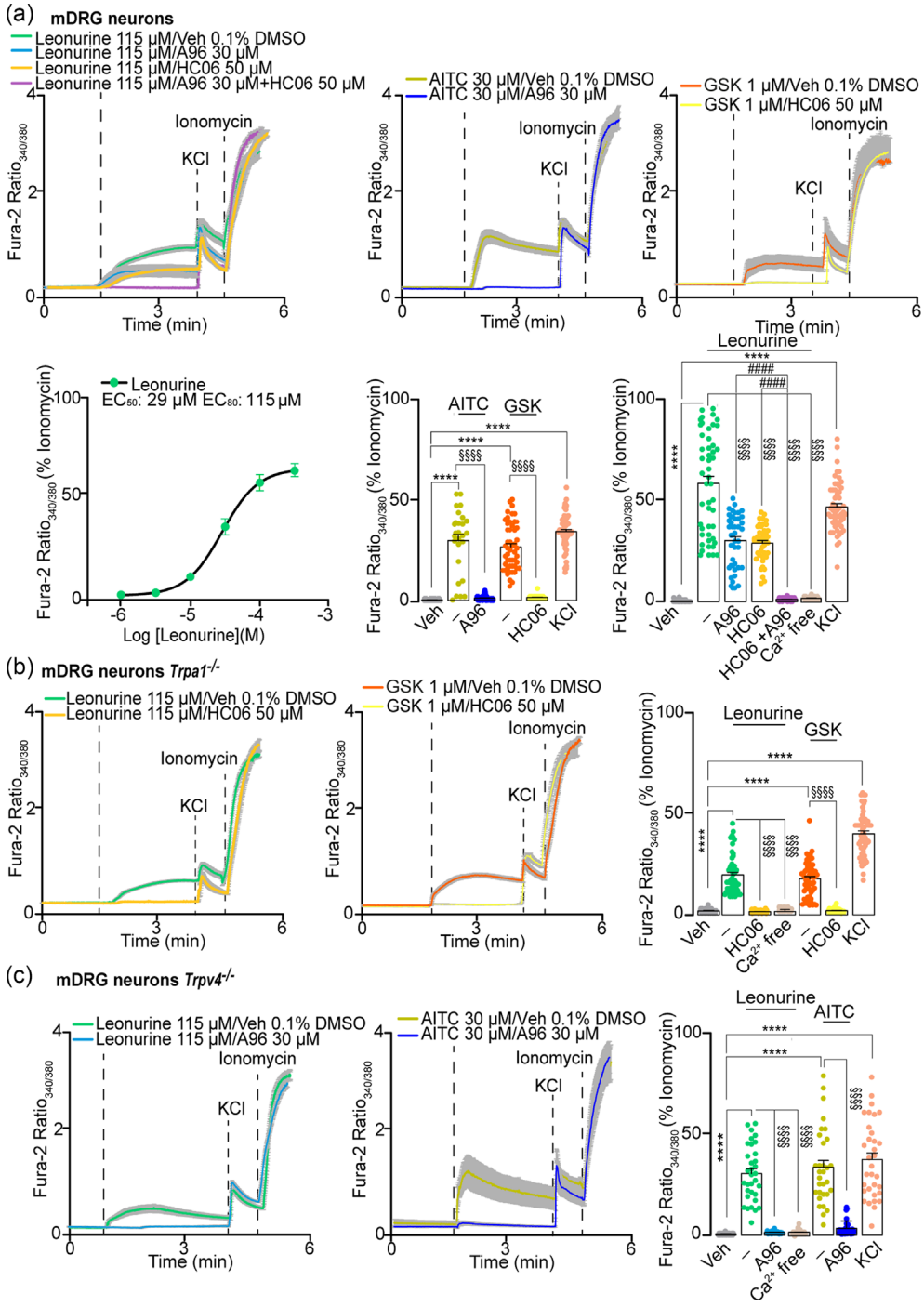

FIGURE 3 **Leonurine activates TRPA1 and TRPV4 channels in mouse DRG neurons.** (a) Typical traces, CRC and cumulative data of Ca^{2+} response in DRG neurons from C57BL/6J mice stimulated with leonurine (CRC cells number: 1 μM $n = 66$, 3 μM $n = 51$, 10 μM $n = 79$, 30 μM $n = 65$, 100 μM $n = 49$, 300 μM $n = 46$; $n = 3$ independent experiments), allyl isothiocyanate (AITC) or GSK1016790A (GSK) in the presence of vehicle (Veh), A967079 (A96), HC067047 (HC06), A96 + HC06 or Ca^{2+}-free medium (cells number: AITC/Veh $n = 27$, AITC/A96 $n = 52$, GSK/ Veh $n = 51$, GSK/HC06 $n = 35$ Veh $n = 42$, KCl $n = 65$; leonurine/Veh $n = 49$, leonurine/A96 $n = 45$, leonurine/HC06 $n = 44$, leonurine/A96 + HC06 $n = 80$, Ca^{2+}-free $n = 42$, Veh $n = 54$, KCl $n = 53$; $n = 3$ independent experiments). (b) Typical traces and cumulative data of Ca^{2+} responses in DRG neurons from *Trpa1*$^{-/-}$ mice stimulated with leonurine or GSK in the presence of Veh, HC06 or Ca^{2+}-free medium (cells number: leonurine/ Veh $n = 57$, leonurine/HC06 $n = 92$, GSK/Veh $n = 56$, GSK/HC06 $n = 51$, Ca^{2+}-free $n = 39$, Veh $n = 51$, KCl $n = 57$; $n = 3$ independent experiments). (c) Typical traces and cumulative data of Ca^{2+} responses in DRG neurons from *Trpv4*$^{-/-}$ mice stimulated with leonurine or AITC in the presence of Veh, A96 or Ca^{2+}-free medium (cells number: leonurine/Veh $n = 33$, leonurine/A96 $n = 53$, AITC/Veh $n = 31$, AITC/A96 $n = 31$, Ca^{2+}-free $n = 35$, Veh $n = 39$, KCl $n = 33$; $n = 3$ independent experiments). In typical trace graphs, the coloured line is the average calcium trace for all cells in a slide, in grey the SEM. Typical traces from different experiments are superimposed to qualitatively show the differences between treatments. The concentration of compounds in the cumulative data graph corresponds to those indicated in the typical traces. Dash (–) is a combination of vehicles. Data are mean ± SEM, one-way ANOVA and Bonferroni correction. **** $P < 0.0001$; §§§§ $P < 0.0001$;#### $P < 0.0001$.

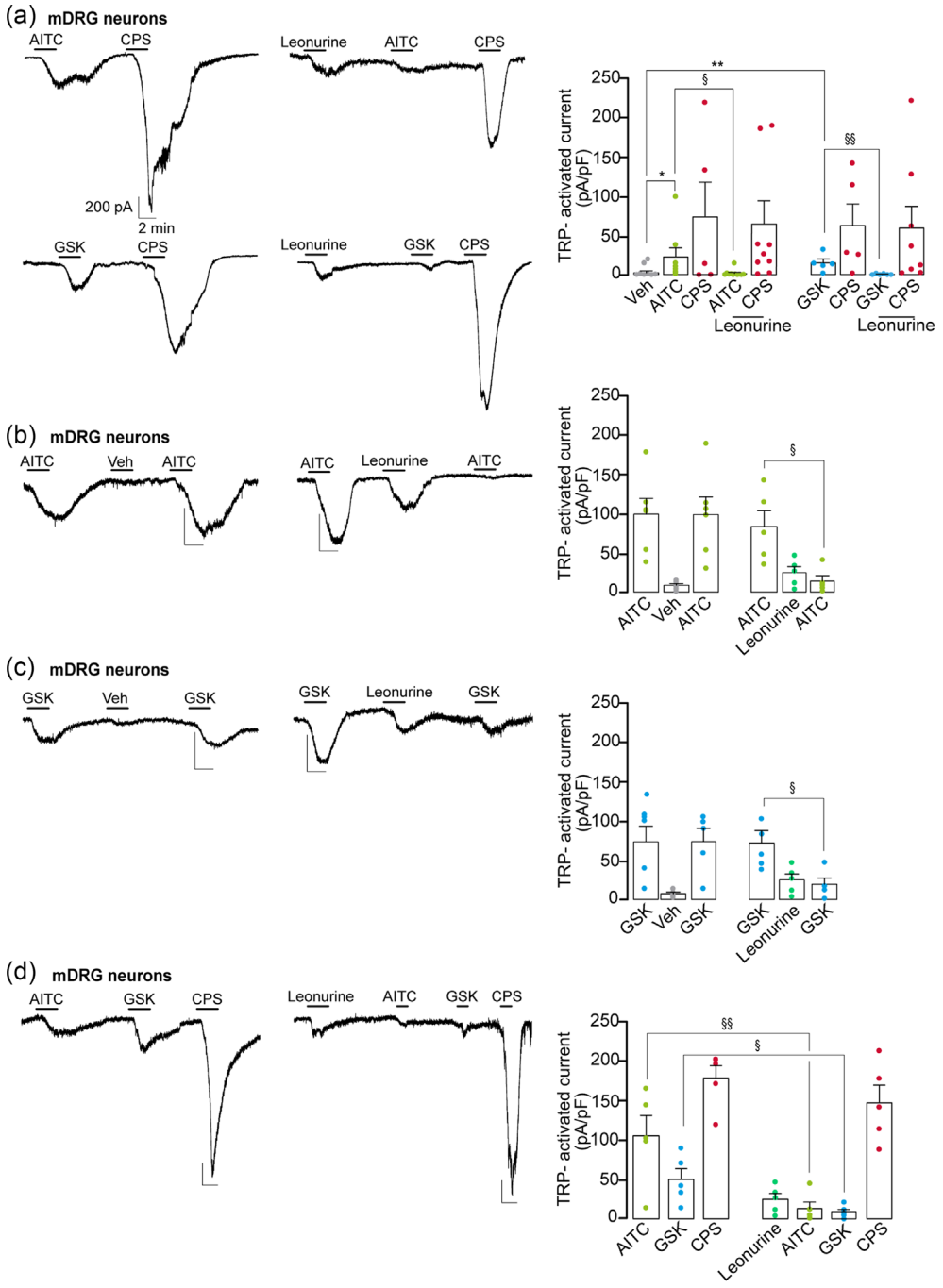

FIGURE 4 **Leonurine activates and desensitises TRPA1 and TRPV4 channels in mouse DRG neurons.** (a) Representative current traces and pooled data of whole-cell patch-clamp inward current in DRG neurons from C57BL/6J mice (mDRG) stimulated with vehicle (Veh, 0.1% DMSO), AITC (200 μM), GSK1016790A (GSK, 10 μM) and CPS, 10 μM) in the presence of leonurine (100 μM) or Veh (cells number: AITC $n = 8$, AITC/CPS $n = 5$, leonurine/AITC $n = 11$, leonurine/AITC/CPS $n = 9$, GSK $n = 5$, GSK/CPS $n = 5$, leonurine/GSK $n = 6$, leonurine/GSK/CPS $= 8$ Veh $n = 8$). (b, c) Representative current traces and pooled data of whole-cell patch-clamp inward current in mDRG neurons evoked by consecutive AITC (200 μM) or GSK (10 μM) applications separated by Veh (0.1% DMSO) or leonurine (100 μM) (cells number: b, AITC $n = 6$, Veh $n = 6$, AITC $n = 6$, AITC $n = 5$, leonurine $n = 5$, AITC $n = 5$; c, GSK $n = 5$, Veh $n = 5$, GSK $n = 5$, GSK $n = 5$, leonurine $n = 5$, GSK $n = 5$). (d) Representative current traces and pooled data of whole-cell patch-clamp inward current in mDRG neurons evoked by AITC (200 μM) and GSK (10 μM) applied consecutively in the absence or presence of leonurine (100 μM) pre-exposure (cells number: AITC $n = 5$, GSK $n = 5$, CPS $n = 5$, leonurine $n = 5$, AITC $n = 5$, GSK $n = 5$, CPS $n = 5$). Data are mean ± SEM, paired Student's *t*-test and unpaired Student's *t*-test. * $P < 0.05$, ** $P < 0.01$, § $P < 0.05$, §§ $P < 0.01$.

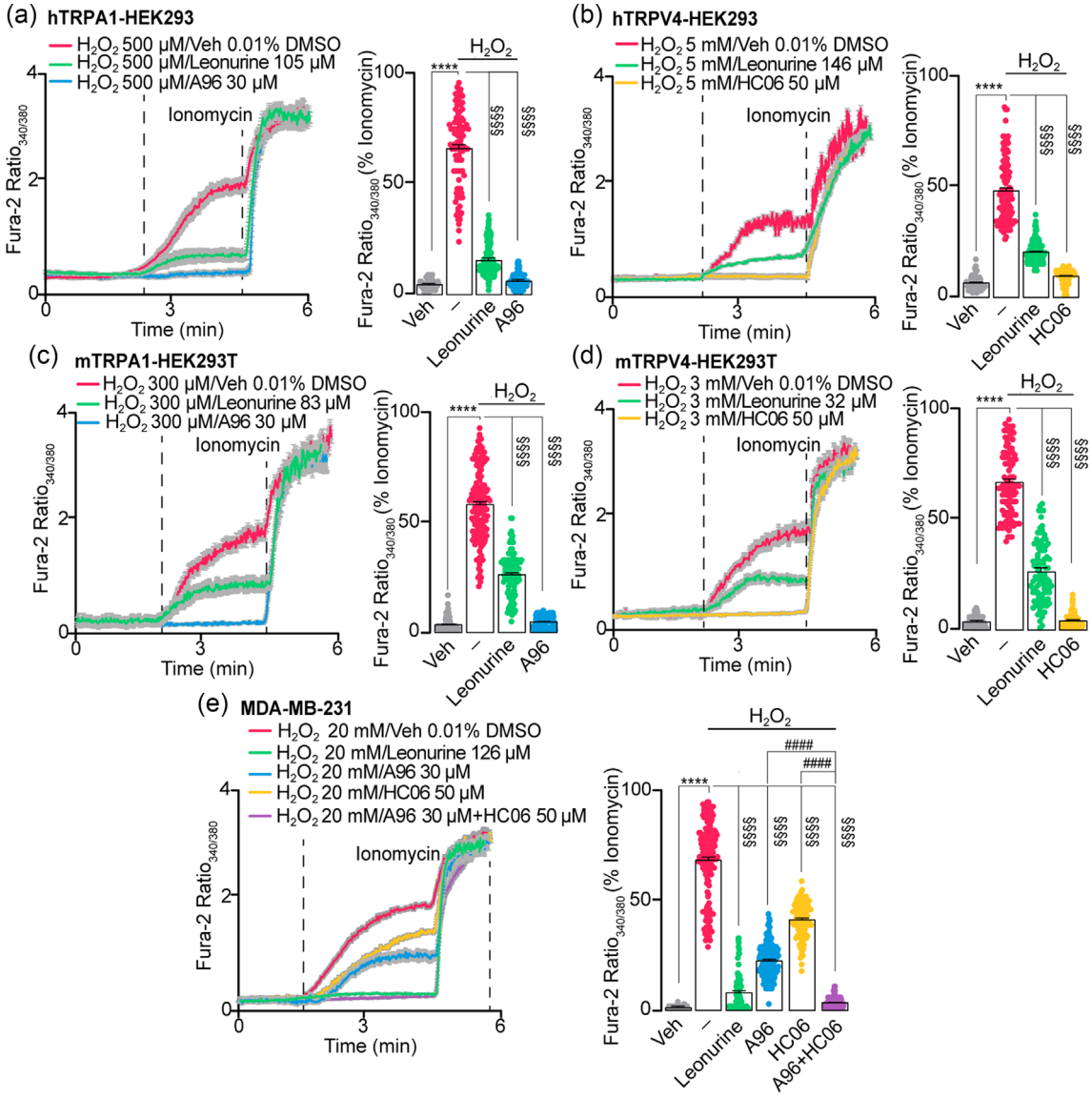

FIGURE 5 **Leonurine modulates the H_2O_2-dependent TRPA1 and TRPV4 channels Ca^{2+} responses.** (a) Typical traces and pooled data of Ca^{2+} responses evoked by hydrogen peroxide H_2O_2 in hTRPA1-HEK293 cells, in the presence of vehicle (Veh), leonurine and A967079 (A96) (cells number: H_2O_2/Veh $n = 99$, H_2O_2/leonurine $n = 209$, H_2O_2/A96 $n = 102$, Veh $n = 101$; $n = 3$ independent experiments). (b) Typical traces and pooled data of Ca^{2+} responses in hTRPV4-HEK293 cells stimulated with H_2O_2 in the presence of Veh, leonurine and HC067047 (HC06) (cells number: H_2O_2/Veh $n = 116$, H_2O_2/leonurine $n = 162$, H_2O_2/HC06 $n = 72$, Veh $n = 49$; $n = 3$ independent experiments). (c) Typical traces and pooled data of Ca^{2+} responses evoked by H_2O_2 in mTRPA1-HEK293T cells, in the presence of Veh, leonurine and A96 (cells number: H_2O_2/Veh $n = 145$, H_2O_2/leonurine $n = 113$, H_2O_2/A96 $n = 173$, Veh $n = 107$; $n = 3$ independent experiments). (d) Typical traces and pooled data of Ca^{2+} responses in mTRPV4-HEK293T cells stimulated with H_2O_2 in the presence of Veh, leonurine or HC06 (cells number: H_2O_2/Veh $n = 108$, H_2O_2/leonurine $n = 96$, H_2O_2/HC06 $n = 182$, Veh $n = 145$; $n = 3$ independent experiments). (e) Typical traces and pooled data of Ca^{2+} responses in MDA-MB-231 cells with H_2O_2 in the presence of Veh, leonurine, A96, HC06 or A96 + HC06 (cells number: H_2O_2/Veh $n = 170$, H_2O_2/leonurine $n = 99$, H_2O_2/A96 $n = 152$, H_2O_2/HC06 $n = 104$, H_2O_2/A96 + HC06 $n = 180$, Veh $n = 101$; $n = 3$ independent experiments). In typical trace graphs, the coloured line is the average calcium trace for all cells in a slide, in grey the SEM. Typical traces from different experiments are superimposed to qualitatively show the differences between treatments. The concentration of compounds in the cumulative data graph corresponds to those indicated in the typical traces. Dash (–) is a combination of vehicles. Data are mean ± SEM, one-way ANOVA and Bonferroni correction. **** $P < 0.0001$; §§§§ $P < 0.0001$; #### $P < 0.0001$.

Here, we showed that the peripheral administration of leonurine (10 nmol, i.pl., once daily from day 1 for seven consecutive days) partially alleviated mechanical allodynia at day 7 following thalidomide administration, when allodynia has reached a plateau (De Logu et al., 2020) (Figure 6f). The same treatment regimen completely abolished the response to a cold stimulus (Figure 6f). Intrathecal leonurine (10 nmol, i.th. once daily from day 1 for seven consecutive days) also partially reduced mechanical allodynia, as well as the cold response

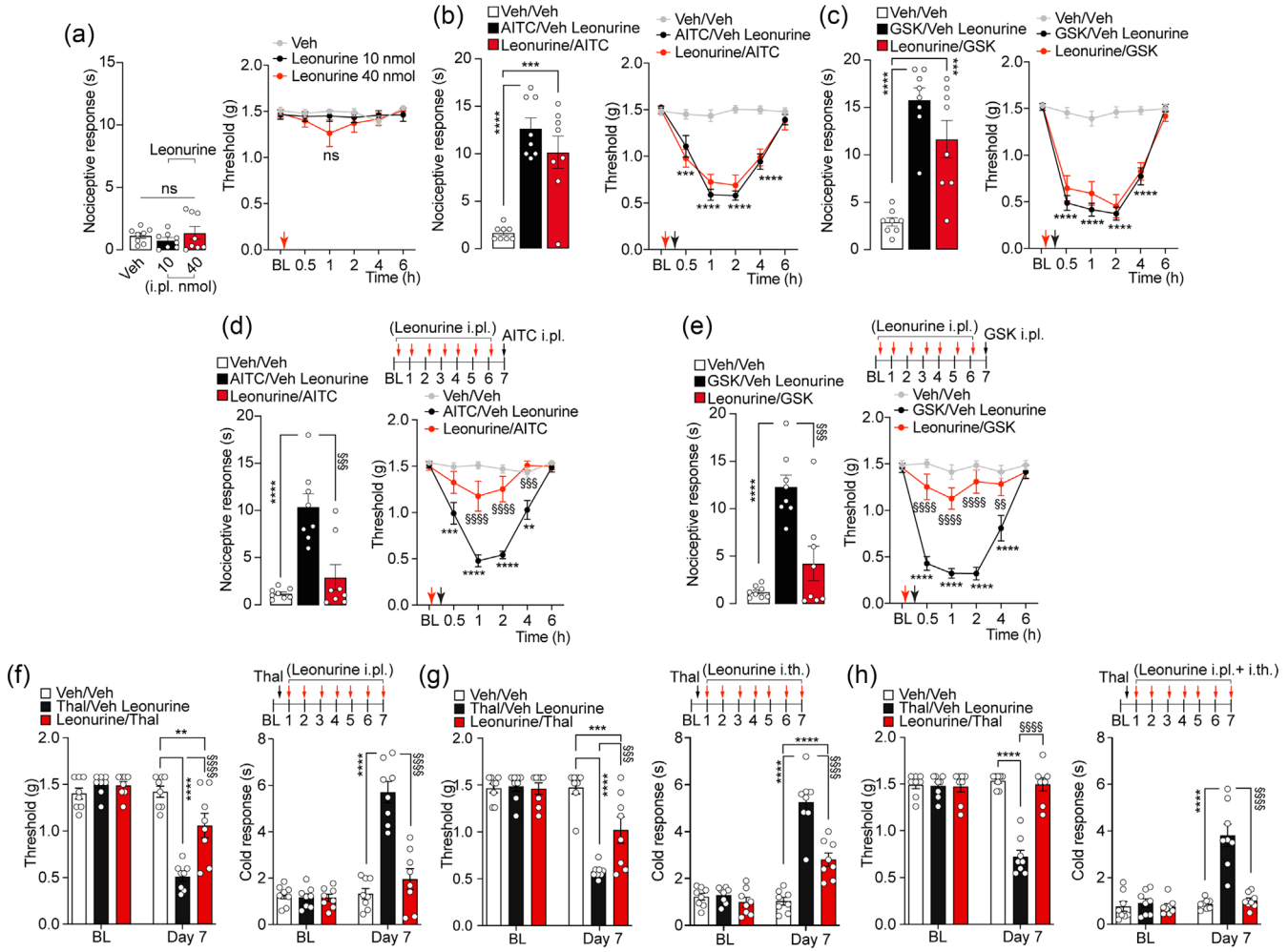

FIGURE 6 **Leonurine desensitises TRPA1 and TRPV4 channels modulating pain responses.** (a) Acute nociceptive response and time-dependent allodynia after intraplantar (i.pl.) leonurine (10, 40 nmol) or vehicle (Veh). (b, c) Acute nociceptive response and time-dependent mechanical allodynia after allyl isothiocyanate (AITC, 10 nmol, i.pl.), GSK1016790A (GSK, 2.5 nmol, i.pl.) or Veh in mice pretreated with leonurine (10 nmol, i.pl., single administration). (d, e) Acute nociceptive response and time-dependent mechanical allodynia after AITC (10 nmol, i.pl.) GSK (2.5 nmol, i.pl.) or Veh in mice pretreated for 7 days with leonurine (10 nmol, i.pl.). Mechanical allodynia and cold response at day 7 after thalidomide (Thal, 50 mg kg^{-1}, intraperitoneal i.p.) or Veh in mice treated for 7 days (day1–day7) with leonurine (10 nmol), (f) i.pl. or (g) intrathecal (i.th) or (h) with a combination i.pl. + i.th. ($n = 8$ mice per group). BL, basal level. Data are mean ± SEM, one-way or two-way ANOVA and Bonferroni correction. * $P < 0.05$, ** $P < 0.01$, *** $P < 0.001$, **** $P < 0.0001$ versus Veh/Veh §§ $P < 0.01$, §§§ $P < 0.001$, §§§§ $P < 0.0001$ versus AITC/Veh leonurine, GSK/Veh leonurine, Thal/Veh leonurine.

(Figure 6g). Notably, the repeated combined administration (i.pl. and i.th.) of leonurine significantly reduced thalidomide-dependent mechanical allodynia and cold response (Figure 6h). In contrast, a single administration of leonurine, whether delivered i.pl., i.th., or in combination, did not affect thalidomide-induced mechanical allodynia and cold response (Figure S3a–c).

To further confirm the specificity of leonurine for TRPA1 and TRPV4 channels in vivo and to exclude off-target effect, we employed a Cre-dependent AAV-mediated neuronal silencing approach. Mice expressing Cre recombinase under the Advillin promoter (Adv-Cre), which drives recombination selectively in sensory neurons, were injected with AAVs encoding a floxed shRNA sequence targeting either *Trpa1* or *Trpv4*, generating Adv-Cre-shRNA (*Trpa1*) and Adv-Cre-shRNA (*Trpv4*) mice, respectively. Knockdown efficiency of each target was verified in DRGs by RT-qPCR (Figure S3d). In Adv-Cre-shRNA (*Trpa1*) mice, 7 days after thalidomide treatment, mechanical allodynia was partially reduced, and cold response was completely prevented compared with control mice, confirming TRPA1's role (De Logu et al., 2020) (Figure 7a). Repeated peripheral administration of leonurine (10 nmol, i.pl., daily for 7 days) did not further reduce mechanical allodynia in Adv-Cre-shRNA (*Trpa1*) mice compared to vehicle-treated mice, excluding off-target effects (Figure 7b). However, mechanical allodynia was fully abolished after intrathecal (i.th.) administration of leonurine (Figure 7c). Furthermore, in Adv-Cre-shRNA (*Trpv4*) mice, mechanical allodynia was partially reduced, but the cold response was not affected, consistent with previous findings (De Logu et al., 2020) (Figure 7d). Repeated intrathecal administration of leonurine did not further reduce mechanical allodynia, again

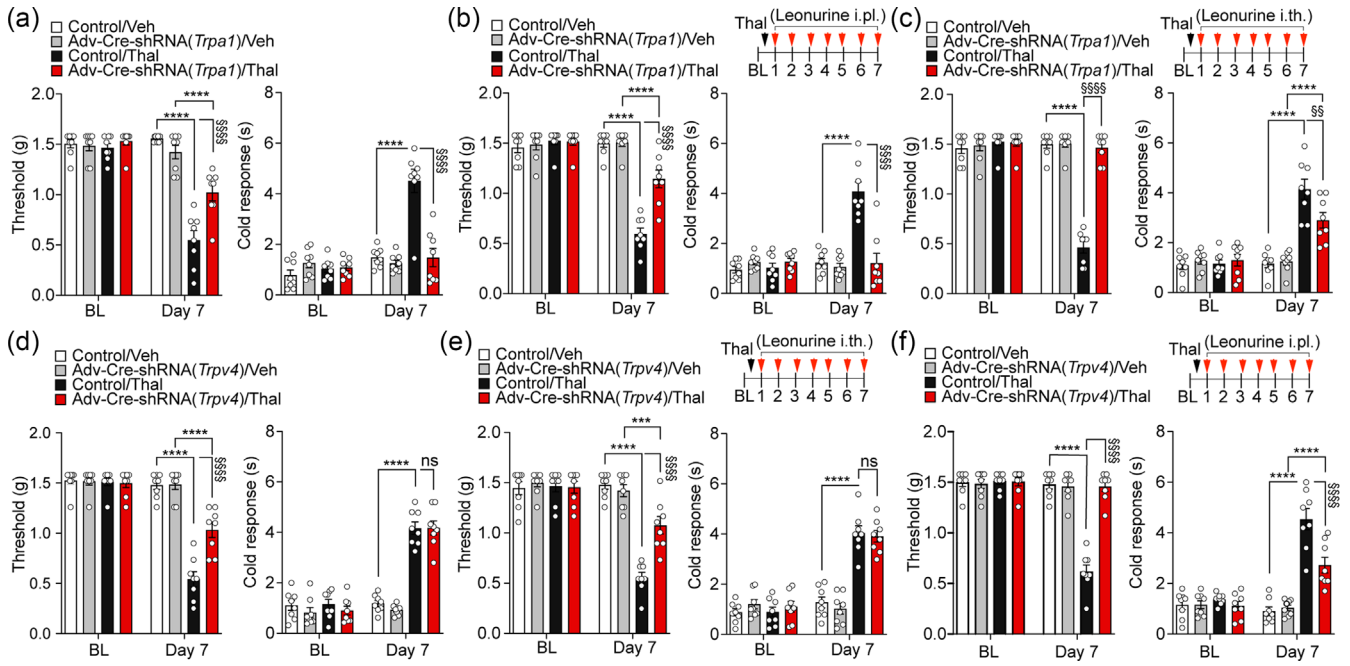

FIGURE 7 **Leonurine specifically targets TRPA1 and TRPV4 channels in vivo.** (a) Mechanical allodynia and cold response at day 7 after thalidomide (Thal, 50 mg kg^{-1}, intraperitoneal i.p.) or Veh in Adv-Cre-shRNA (*Trpa1*) or control mice. Mechanical allodynia and cold response at day 7 after thalidomide (Thal, 50 mg kg^{-1}, i.p.) or Veh in Adv-Cre-shRNA (*Trpa1*) or control mice treated for 7 days (day1–day7) with leonurine (10 nmol), (b) intraplantar (i.pl) or (c) intrathecal (i.th). (d) Mechanical allodynia and cold response at day 7 after Thal (50 mg kg^{-1}, i.p.) or Veh in Adv-Cre-shRNA (*Trpv4*) or control mice. Mechanical allodynia and cold response at day 7 after thalidomide (Thal, 50 mg kg^{-1}, i.p.) or Veh in Adv-Cre-shRNA (*Trpv4*) or control mice treated for 7 days (day1–day7) with leonurine (10 nmol), (e) i.th. or (f) i.pl. ($n = 8$ mice per group). BL, basal level. Data are mean ± SEM, two-way ANOVA and Bonferroni correction. *** $P < 0.001$, **** $P < 0.0001$, §§ $P < 0.01$, §§§§ $P < 0.0001$.

confirming the absence of off-target effects (Figure 7e). However, mechanical allodynia was abolished following peripheral (i.pl.) leonurine administration (Figure 7f). Altogether, these data provide evidence for specific action of leonurine through TRPA1 and TRPV4 channels in alleviating pain in CIPN model.

4 | DISCUSSION

The pharmacological and genetic evidence presented supports the therapeutic potential of leonurine, highlighting its activation and desensitisation of the redox-sensitive ion channels TRPA1 and TRPV4. At the molecular level, both TRPA1 and TRPV4 are activated with similar efficiency in native and recombinant cells derived from mice and humans, indicating that the effect of the compound observed in the rodent channel isoform may be replicated in the human counterpart. Notably, leonurine does not activate the TRPV1 channel, indicating that its ability to activate nociceptors is mediated through the selective targeting of TRPA1 and TRPV4.

Primary sensory neurons that express TRP channels are essential for detecting a range of stimuli, including temperature (heat and cold), taste and pain. The mechanism of action of leonurine is similar to that of AITC for TRPA1 and GSK for TRPV4; however, its lower efficacy suggests that leonurine may function as a partial agonist of these channels. As previously observed with the herbal compounds, isopetasin (Benemei et al., 2017) and **parthenolide** (Trevisan et al., 2013), leonurine induces desensitisation of primary sensory neurons. However, unlike these compounds, which selectively target the TRPA1 channel, leonurine desensitises nociceptors through the dual activation of both TRPA1 and TRPV4 channels.

Among the more than 280 secondary metabolites isolated from *Leonurus*, including alkaloids, terpenes and flavonoids (Liu et al., 2024; Suguro et al., 2018), leonurine is recognised as the primary bioactive metabolite (Liu et al., 2012). In traditional Chinese medicine, leonurine is widely used to manage a variety of inflammatory conditions including menstrual disorders, neuroinflammation, cardiovascular inflammation and postpartum abdominal pain (Kuchta et al., 2010). These therapeutic effects are primarily attributed to leonurine's potent antioxidant properties (Zhang et al., 2012; Zhu et al., 2018). By scavenging free radicals and enhancing the expression of antioxidant enzymes, including superoxide dismutase and glutathione peroxidase (Sun et al., 2005; Zheng et al., 2023), leonurine reduces oxidative stress, resulting in alleviating inflammation and preventing tissue damage (Deng et al., 2022; Landini, Monteiro, et al., 2023).

ROS play a crucial role in chronic pain development and maintenance. Tissue damage has been shown to promote ROS production, which, through neuronal interactions and mitochondrial dysfunction, contributes to various pain pathways (Beckhauser et al., 2016). Recently, we observed that ROS play a significant role in chronic pain modulation by activating TRP channels, primarily TRPA1 and TRPV4,

in both neuronal and non-neuronal cells (De Logu et al., 2020). In a mouse model of neuropathic pain induced by partial sciatic nerve ligation, ROS-induced activation of TRPA1 on Schwann cells initiates a feedforward mechanism that promotes macrophage accumulation at the neuronal level, ultimately contributing to the establishment and maintenance of a persistent chronic pain state (De Logu et al., 2017). This mechanism has been confirmed in other chronic pain mouse models, including alcoholic neuropathy (De Logu et al., 2019), cancer (De Logu et al., 2021; Landini, Marini, et al., 2023), migraine (De Logu et al., 2022; Landini, Monteiro, et al., 2023) and endometriosis (Titiz et al., 2024). Similarly, TRPV4 has been implicated in several pain mechanisms associated with ROS production, such as neuropathic pain induced by chronic compression of the dorsal root ganglia (Rodrigues et al., 2022; Wang et al., 2011, 2015) and diabetic neuropathy (Osmanlioglu & Naziroglu, 2024).

Chronic CIPN is a prevalent and debilitating side effect associated with various anticancer drugs, significantly impacting patients' quality of life and often leading to treatment discontinuation or dose reduction (Colvin, 2019). Various rodent models of CIPN have revealed the involvement of different TRP ion channels in the development of this condition. For instance, TRPV1 has been shown to be overexpressed in rodent models of CIPN, playing a key role in modulating thermal hyperalgesia (Boyette-Davis et al., 2015; Hara et al., 2013). Additionally, activation of **TRPM8** has demonstrated clinical evidence of analgesic effects in CIPN (Fallon et al., 2015; Li et al., 2022; Proudfoot et al., 2006). Our research further revealed that TRPA1 and TRPV4 act synergistically in thalidomide-induced sensory neuropathy. Notably, the mechanical allodynia induced by a single administration of thalidomide was only partially alleviated when TRPA1 or TRPV4 antagonists were used individually. However, the concurrent administration of both antagonists completely abolished the mechanical allodynia, underscoring their cooperative role in mediating this type of neuropathic pain (De Logu et al., 2020).

Here, a mouse model of CIPN induced by thalidomide was used to investigate the dual role of leonurine in TRPA1- and TRPV4-dependent neuronal desensitisation. Initially, the in vivo effects of leonurine were assessed by evaluating hypersensitivity following intraplantar administration of TRPA1 and TRPV4 selective agonists (AITC and GSK). The results demonstrated that a single dose of leonurine did not alter nociceptive behaviour and ensuing mechanical allodynia induced by either AITC or GSK. However, a significant inhibition of hypersensitivity was observed after a 7-day cycle of leonurine administration, indicating that prolonged treatment is necessary to achieve effective neuronal desensitisation. Subsequently, the 7-day treatment regimen was applied to the thalidomide-induced CIPN mouse model. Remarkably, this extended administration of leonurine led to a significant reduction in mechanical allodynia/cold response associated with thalidomide-induced peripheral neuropathy, demonstrating its efficacy in alleviating neuropathic pain symptoms. Additional data in mice with selective deletion of TRPA1 or TRPV4 in primary sensory neurons further confirmed the contribution of these channels to pain signalling in this model excluding off-target effects of leonurine.

Overall, our findings demonstrate that repeated administration of leonurine leads to a significant reduction in nociceptive behaviours, supporting its ability to induce functional desensitisation of TRPA1 and TRPV4 channels. However, given the complexity of in vivo pain signalling, we cannot exclude the involvement of additional mechanisms, such as oxidative stress modulation, neuroimmune interactions or effects on other pain-related receptors. This limitation, inherent to behavioural pharmacology, highlights the need for further mechanistic studies to fully elucidate the pathways underlying leonurine's analgesic effects. Nonetheless, the dual targeting of TRPA1 and TRPV4 by leonurine, together with its antioxidant properties, remarks the compound as a promising candidate for the treatment of CIPN and other chronic pain syndromes.

5 | CONCLUSIONS

In conclusion, our study provides compelling evidence that leonurine exerts significant chronic pain control in a mouse model of CIPN through its dual action as a partial agonist of both TRPA1 and TRPV4 receptors, facilitating neuronal desensitisation. Importantly, the effectiveness of leonurine is dependent on a prolonged treatment regimen rather than acute administration, highlighting the necessity of sustained exposure to achieve therapeutic benefits. These findings position leonurine as a promising candidate for pain management strategies that target redox-sensitive ion channels involved in sensory processing. Future studies should focus on elucidating the precise molecular mechanisms underlying leonurine's dual action on TRPA1 and TRPV4, optimising its dosing regimens, and assessing its therapeutic potential in animal models that better mimic human diseases for which leonurine is traditionally used in Chinese medicine, such as inflammatory disorders and neuropathic pain. Investigating leonurine's long-term safety profile, pharmacokinetics and potential synergistic effects with existing analgesic therapies also will be crucial in advancing its clinical translation for effective pain management.

AUTHOR CONTRIBUTIONS

M. Marini: Investigation; methodology; writing—original draft. **L. Landini**: Investigation; methodology; writing—original draft. **M. Tesi**: Investigation; methodology; writing—original draft. **E. Coppi**: Investigation; methodology; writing—original draft; formal analysis. **E. Bellantoni**: Methodology. **M. Chieca**: Methodology. **E. B. Croce**: Investigation; methodology. **L. Bonacchi**: Investigation; methodology. **G. Brancolini**: Investigation; methodology. **P. Bruschi**: Data curation. **D. S. M. de Araújo**: Investigation; methodology. **G. De Siena**: Investigation; methodology. **A. Dimitrova**: Investigation; methodology. **A. Mastricci**: Investigation; methodology. **H. RochaMendonça**: Investigation; methodology. **I. Scuffi**: Investigation; methodology. **M. Venturini**: Investigation; methodology. **L. Dos Santos Heringer**: Investigation; methodology. **F. Vaiano**: Conceptualisation; investigation; data curation. **R. Nassini**: Conceptualisation; project administration; writing—original draft; writing—review and editing; funding

acquisition. **F. De Logu**: Conceptualisation; project administration; writing—original draft; writing—review and editing and Funding acquisition.

ACKNOWLEDGEMENTS

We thank A.H. Morice, University of Hull, Hull, UK for hTRPA1-HEK293, and M.J. Gunthorpe, GlaxoSmithKline, Harlow, UK for hTRPV1-HEK293. Views and opinions expressed are, however, those of the author(s) only and do not necessarily reflect those of the European Union or the European Commission. Neither the European Union nor the European Commission can be held responsible for them. Open access publishing facilitated by Universita degli Studi di Firenze, as part of the Wiley - CRUI-CARE agreement.

CONFLICT OF INTEREST STATEMENT

R.N. and F.D.L. are founding scientists of FloNext Srl. G.B. is fully employed at FloNext Srl, Italy. All other authors declare that they have no competing interests.

DATA AVAILABILITY STATEMENT

Data will be made available on request from corresponding authors.

DECLARATION OF TRANSPARENCY AND SCIENTIFIC RIGOUR

This Declaration acknowledges that this paper adheres to the principles for transparent reporting and scientific rigour of preclinical research as stated in the BJP guidelines for Design and Analysis, and Animal Experimentation and as recommended by funding agencies, publishers and other organisations engaged with supporting research.

ORCID

Romina Nassini https://orcid.org/0000-0002-9223-8395

REFERENCES

Al-Anzi, B., Tracey, W. D. Jr., & Benzer, S. (2006). Response of Drosophila to wasabi is mediated by painless, the fly homolog of mammalian TRPA1/ANKTM1. *Curr Biol*, *16*, 1034–1040. https://doi.org/10.1016/j.cub.2006.04.002

Alexander, S. P. H., Fabbro, D., Kelly, E., Mathie, A. A., Peters, J. A., Veale, E. L., Armstrong, J. F., Faccenda, E., Harding, S. D., Davies, J. A., Annett, S., Boison, D., Burns, K. E., Dessauer, C., Gertsch, J., Helsby, N. A., Izzo, A. A., Ostrom, R., Papapetropoulos, A., … Wong, S. S. (2023). The concise guide to PHARMACOLOGY 2023/24: Enzymes. *British Journal of Pharmacology*, *180*(Suppl 2), S289–S373. https://doi.org/10.1111/bph.16181

Andersson, D. A., Gentry, C., Moss, S., & Bevan, S. (2008). Transient receptor potential A1 is a sensory receptor for multiple products of oxidative stress. *J Neurosci*, *28*, 2485–2494. https://doi.org/10.1523/JNEUROSCI.5369-07.2008

Beckhauser, T. F., Francis-Oliveira, J., & De Pasquale, R. (2016). Reactive oxygen species: Physiological and physiopathological effects on synaptic plasticity. *J Exp Neurosci*, *10*, 23–48. https://doi.org/10.4137/JEN.S39887

Bellantoni, E., Marini, M., Chieca, M., Gabellini, C., Crapanzano, E. L., Monteiro, S., de Araujo, D., Nosi, D., Roschi, L., Landini, L., De Siena, G., Pensieri, P., Mastricci, A., Scuffi, I., Geppetti, P., Nassini, R., & De Logu, F. (2024). Schwann cell transient receptor potential ankyrin 1 (TRPA1) ortholog in zebrafish larvae mediates chemotherapy-induced peripheral neuropathy. *British Journal of Pharmacology*, *181*, 4859–4873. https://doi.org/10.1111/bph.17318

Benemei, S., De Logu, F., Li Puma, S., Marone, I. M., Coppi, E., Ugolini, F., Liedtke, W., Pollastro, F., Appendino, G., Geppetti, P., Materazzi, S., & Nassini, R. (2017). The anti-migraine component of butterbur extracts, isopetasin, desensitizes peptidergic nociceptors by acting on TRPA1 cation channel. *British Journal Pharmacology*, *174*, 2897–2911. https://doi.org/10.1111/bph.13917

Bera, K., Kiepas, A., Godet, I., Li, Y., Mehta, P., Ifemembi, B., Paul, C. D., Sen, A., Serra, S. A., Stoletov, K., Tao, J., Shatkin, G., Lee, S. J., Zhang, Y., Boen, A., Mistriotis, P., Gilkes, D. M., Lewis, J. D., Fan, C. M., … Konstantopoulos, K. (2022). Extracellular fluid viscosity enhances cell migration and cancer dissemination. *Nature*, *611*, 365–373. https://doi.org/10.1038/s41586-022-05394-6

Boiko, N., Medrano, G., Montano, E., Jiang, N., Williams, C. R., Madungwe, N. B., Bopassa, J. C., Kim, C. C., Parrish, J. Z., Hargreaves, K. M., Stockand, J. D., & Eaton, B. A. (2017). TrpA1 activation in peripheral sensory neurons underlies the ionic basis of pain hypersensitivity in response to vinca alkaloids. *PLoS ONE*, *12*, e0186888. https://doi.org/10.1371/journal.pone.0186888

Boyette-Davis, J. A., Walters, E. T., & Dougherty, P. M. (2015). Mechanisms involved in the development of chemotherapy-induced neuropathy. *Pain Management*, *5*, 285–296. https://doi.org/10.2217/pmt.15.19

Cameron, N. E., Eaton, S. E., Cotter, M. A., & Tesfaye, S. (2001). Vascular factors and metabolic interactions in the pathogenesis of diabetic neuropathy. *Diabetologia*, *44*, 1973–1988. https://doi.org/10.1007/s001250100001

Cao, D. S., Yu, S. Q., & Premkumar, L. S. (2009). Modulation of transient receptor potential vanilloid 4-mediated membrane currents and synaptic transmission by protein kinase C. *Molecular Pain*, *5*, 5. https://doi.org/10.1186/1744-8069-5-5

Chaplan, S. R., Bach, F. W., Pogrel, J. W., Chung, J. M., & Yaksh, T. L. (1994). Quantitative assessment of tactile allodynia in the rat paw. *J Neurosci Methods*, *53*, 55–63. https://doi.org/10.1016/0165-0270(94)90144-9

Colvin, L. A. (2019). Chemotherapy-induced peripheral neuropathy: Where are we now? *Pain*, *160*(Suppl 1), S1–S10. https://doi.org/10.1097/j.pain.0000000000001540

Curtis, M. J., Alexander, S., Cirino, G., Docherty, J. R., George, C. H., Giembycz, M. A., Hoyer, D., Insel, P. A., Izzo, A. A., Ji, Y., MacEwan, D. J., Sobey, C. G., Stanford, S. C., Teixeira, M. M., Wonnacott, S., & Ahluwalia, A. (2018). Experimental design and analysis and their reporting II: Updated and simplified guidance for authors and peer reviewers. *British Journal of Pharmacology*, *175*, 987–993. https://doi.org/10.1111/bph.14153

De Logu, F., Li Puma, S., Landini, L., Portelli, F., Innocenti, A., de Araujo, D. S. M., Janal, M. N., Patacchini, R., Bunnett, N. W., Geppetti, P., & Nassini, R. (2019). Schwann cells expressing nociceptive channel TRPA1 orchestrate ethanol-evoked neuropathic pain in mice. *Journal of Clinical Investigation*, *129*, 5424–5441. https://doi.org/10.1172/JCI128022

De Logu, F., Marini, M., Landini, L., Monteiro, S., de Araujo, D., Bartalucci, N., Trevisan, G., Bruno, G., Marangoni, M., Schmidt, B. L., Bunnett, N. W., & Geppetti, P. (2021). Peripheral nerve resident macrophages and Schwann cells mediate cancer-induced pain. *Cancer Research*, *81*, 3387–3401. https://doi.org/10.1158/0008-5472.CAN-20-3326

De Logu, F., Nassini, R., Hegron, A., Landini, L., Jensen, D. D., Latorre, R., Ding, J., Marini, M., Souza Monteiro de Araujo, D., Ramírez-Garcia, P., & Whittaker, M. (2022). Schwann cell endosome CGRP signals elicit periorbital mechanical allodynia in mice. *Nature Communications*, *13*, 646. https://doi.org/10.1038/s41467-022-28204-z

De Logu, F., Nassini, R., Materazzi, S., Carvalho Goncalves, M., Nosi, D., Rossi Degl'Innocenti, D., Marone, I. M., Ferreira, J., Li Puma, S., Benemei, S., & Trevisan, G. (2017). Schwann cell TRPA1 mediates neuroinflammation that sustains macrophage-dependent neuropathic pain in mice. *Nature Communications*, *8*, 1887.

De Logu, F., Tonello, R., Materazzi, S., Nassini, R., Fusi, C., Coppi, E., Li Puma, S., Marone, I. M., Sadofsky, L. R., Morice, A. H., & Susini, T. (2016). TRPA1 mediates aromatase inhibitor-evoked pain by the aromatase substrate androstenedione. *Cancer Research*, *76*, 7024–7035. https://doi.org/10.1158/0008-5472.CAN-16-1492

De Logu, F., Trevisan, G., Marone, I. M., Coppi, E., Padilha Dalenogare, D., Titiz, M., Marini, M., Landini, L., Souza Monteiro de Araujo, D., Li Puma, S., & Materazzi, S. (2020). Oxidative stress mediates thalidomide-induced pain by targeting peripheral TRPA1 and central TRPV4. *BMC Biology*, *18*, 197. https://doi.org/10.1186/s12915-020-00935-9

Deng, Z., Li, J., Tang, X., Li, D., Wang, Y., Wu, S., Fan, K., & Ma, Y. (2022). Leonurine reduces oxidative stress and provides neuroprotection against ischemic injury via modulating oxidative and NO/NOS pathway. *International Journal of Molecular Sciences*, *23*, 10188. https://doi.org/10.3390/ijms231710188

Fallon, M. T., Storey, D. J., Krishan, A., Weir, C. J., Mitchell, R., Fleetwood-Walker, S. M., Scott, A. C., & Colvin, L. A. (2015). Cancer treatment-related neuropathic pain: Proof of concept study with menthol—A TRPM8 agonist. *Supportive Care in Cancer*, *23*, 2769–2777. https://doi.org/10.1007/s00520-015-2642-8

Faul, F., Erdfelder, E., Lang, A. G., & Buchner, A. (2007). G*power 3: A flexible statistical power analysis program for the social, behavioral, and biomedical sciences. *Behavior Research Methods*, *39*, 175–191. https://doi.org/10.3758/BF03193146

Girard, B. M., Merrill, L., Malley, S., & Vizzard, M. A. (2013). Increased TRPV4 expression in urinary bladder and lumbosacral dorsal root ganglia in mice with chronic overexpression of NGF in urothelium. *Journal of Molecular Neuroscience*, *51*, 602–614. https://doi.org/10.1007/s12031-013-0033-5

Guler, A. D., Lee, H., Iida, T., Shimizu, I., Tominaga, M., & Caterina, M. (2002). Heat-evoked activation of the ion channel, TRPV4. *The Journal of Neuroscience*, *22*, 6408–6414. https://doi.org/10.1523/JNEUROSCI.22-15-06408.2002

Han, S., Tie, X., Meng, L., Wang, Y., & Wu, A. (2013). PMA and ionomycin induce glioblastoma cell death: Activation-induced cell-death-like phenomena occur in glioma cells. *PLoS ONE*, *8*, e76717. https://doi.org/10.1371/journal.pone.0076717

Hara, T., Chiba, T., Abe, K., Makabe, A., Ikeno, S., Kawakami, K., Utsunomiya, I., Hama, T., & Taguchi, K. (2013). Effect of paclitaxel on transient receptor potential vanilloid 1 in rat dorsal root ganglion. *Pain*, *154*, 882–889. https://doi.org/10.1016/j.pain.2013.02.023

Huang, L., Xu, D. Q., Chen, Y. Y., Yue, S. J., & Tang, Y. P. (2021). Leonurine, a potential drug for the treatment of cardiovascular system and central nervous system diseases. *Brain and Behavior*, *11*, e01995. https://doi.org/10.1002/brb3.1995

Jordt, S. E., Bautista, D. M., Chuang, H. H., McKemy, D. D., Zygmunt, P. M., Hogestatt, E. D., Meng, I. D., & Julius, D. (2004). Mustard oils and cannabinoids excite sensory nerve fibres through the TRP channel ANKTM1. *Nature*, *427*, 260–265. https://doi.org/10.1038/nature02282

Kilkenny, C., Browne, W., Cuthill, I. C., Emerson, M., & Altman, D. G. (2010). Animal research: Reporting in vivo experiments: The ARRIVE guidelines. *British Journal of Pharmacology*, *160*, 1577–1579. https://doi.org/10.1111/j.1476-5381.2010.00872.x

Kim, S., Barry, D. M., Liu, X. Y., Yin, S., Munanairi, A., Meng, Q. T., Cheng, W., Mo, P., Wan, L., Liu, S. B., Ratnayake, K., Zhao, Z. Q., Gautam, N., Zheng, J., Karunarathne, W. K., & Chen, Z. F. (2016). Facilitation of TRPV4 by TRPV1 is required for itch transmission in some sensory neuron populations. *Science Signaling*, *9*, ra71. https://doi.org/10.1126/scisignal.aaf1047

Kuchta, K., Ortwein, J., Briel, D., & Rauwald, H. (2010). Leonurine in *Leonurus* and *Leonotis* drugs? Detection and quantitative determination by a newly developed HPLC method. *Planta Medica*, *76*, P541. https://doi.org/10.1055/s-0030-1264839

Landini, L., Marini, M., Monteiro, S., de Araujo, D., Romitelli, A., Montini, M., Albanese, V., Titiz, M., Innocenti, A., Bianchini, F., Geppetti, P., & Nassini, R. (2023). Schwann cell insulin-like growth factor receptor type-1 mediates metastatic bone cancer pain in mice. *Brain, Behavior, and Immunity*, *110*, 348–364. https://doi.org/10.1016/j.bbi.2023.03.013

Landini, L., Monteiro, S., de Araujo, D., Chieca, M., De Siena, G., Bellantoni, E., Geppetti, P., Nassini, R., & De Logu, F. (2023). Acetaldehyde via CGRP receptor and TRPA1 in Schwann cells mediates ethanol-evoked periorbital mechanical allodynia in mice: Relevance for migraine. *Journal of Biomedical Science*, *30*, 28. https://doi.org/10.1186/s12929-023-00922-6

Landini, L., Monteiro, S., de Araujo, D., Titiz, M., Geppetti, P., Nassini, R., & De Logu, F. (2022). TRPA1 role in inflammatory disorders: What is known so far? *International Journal of Molecular Sciences*, *23*, 4529. https://doi.org/10.3390/ijms23094529

Li, Z., Zhang, H., Wang, Y., Li, Y., Li, Q., & Zhang, L. (2022). The distinctive role of menthol in pain and analgesia: Mechanisms, practices, and advances. *Frontiers in Molecular Neuroscience*, *15*, 1006908. https://doi.org/10.3389/fnmol.2022.1006908

Liedtke, W., Choe, Y., Marti-Renom, M. A., Bell, A. M., Denis, C. S., Sali, A., Hudspeth, A. J., Friedman, J. M., & Heller, S. (2000). Vanilloid receptor-related osmotically activated channel (VR-OAC), a candidate vertebrate osmoreceptor. *Cell*, *103*, 525–535. https://doi.org/10.1016/s0092-8674(00)00143-4

Liedtke, W., & Friedman, J. M. (2003). Abnormal osmotic regulation in trpv4−/− mice. *Proceedings of the National Academy of Sciences of the United States of America*, *100*, 13698–13703. https://doi.org/10.1073/pnas.1735416100

Lilley, E., Stanford, S. C., Kendall, D. E., Alexander, S. P. H., Cirino, G., Docherty, J. R., George, C. H., Insel, P. A., Izzo, A. A., Ji, Y., Panettieri, R. A., Sobey, C. G., Stefanska, B., Stephens, G., Teixeira, M., & Ahluwalia, A. (2020). ARRIVE 2.0 and the British Journal of Pharmacology: Updated guidance for 2020. *British Journal of Pharmacology*, *177*, 3611–3616. https://doi.org/10.1111/bph.15178

Lin, Y. K., Li, Y. Y., Li, Y., Li, D. J., Wang, X. L., Wang, L., Yu, M., Zhu, Y. Z., Cheng, J. J., & Du, M. R. (2022). SCM-198 prevents endometriosis by reversing low autophagy of endometrial stromal cell via balancing ERalpha and PR signals. *Frontiers in Endocrinology*, *13*, 858176.

Liu, H., Zhang, X., Du, Y., Ji, H., Li, S., Li, L., Xing, Y., Zhang, X., Dong, L., Wang, C., & Zhao, K. (2012). Leonurine protects brain injury by increased activities of UCP4, SOD, CAT and Bcl-2, decreased levels of MDA and Bax, and ameliorated ultrastructure of mitochondria in experimental stroke. *Brain Research*, *1474*, 73–81. https://doi.org/10.1016/j.brainres.2012.07.028

Liu, S., Sun, C., Tang, H., Peng, C., & Peng, F. (2024). Leonurine: A comprehensive review of pharmacokinetics, pharmacodynamics, and toxicology. *Frontiers in Pharmacology*, *15*, 1428406. https://doi.org/10.3389/fphar.2024.1428406

Materazzi, S., Benemei, S., Fusi, C., Gualdani, R., De Siena, G., Vastani, N., Moncelli, M. R., Wei, X., & Dussor, G. (2013). Parthenolide inhibits nociception and neurogenic vasodilatation in the trigeminovascular system by targeting the TRPA1 channel. *Pain*, *154*, 2750–2758. https://doi.org/10.1016/j.pain.2013.08.002

Materazzi, S., Fusi, C., Benemei, S., Pedretti, P., Patacchini, R., Nilius, B., Prenen, J., Creminon, C., Geppetti, P., & Nassini, R. (2012). TRPA1 and

TRPV4 mediate paclitaxel-induced peripheral neuropathy in mice via a glutathione-sensitive mechanism. *Pflügers Archiv-European Journal of Physiology*, *463*, 561–569. https://doi.org/10.1007/s00424-011-1071-x

McGrath, J. C., & Lilley, E. (2015). Implementing guidelines on reporting research using animals (ARRIVE etc.): New requirements for publication in BJP. *British Journal of Pharmacology*, *172*, 3189–3193. https://doi.org/10.1111/bph.12955

Mendoza, S. A., Fang, J., Gutterman, D. D., Wilcox, D. A., Bubolz, A. H., Li, R., Suzuki, M., & Zhang, D. X. (2010). TRPV4-mediated endothelial Ca2+ influx and vasodilation in response to shear stress. *American Journal of Physiology Heart and Circulatory Physiology*, *298*, H466–H476. https://doi.org/10.1152/ajpheart.00854.2009

Mori, Y., Takahashi, N., Polat, O. K., Kurokawa, T., Takeda, N., & Inoue, M. (2016). Redox-sensitive transient receptor potential channels in oxygen sensing and adaptation. *Pflugers Archiv*, *468*, 85–97. https://doi.org/10.1007/s00424-015-1716-2

Nagata, K., Duggan, A., Kumar, G., & García-Añoveros, J. (2005). Nociceptor and hair cell transducer properties of TRPA1, a channel for pain and hearing. *The Journal of Neuroscience*, *25*, 4052–4061. https://doi.org/10.1523/JNEUROSCI.0013-05.2005

Nassini, R., Materazzi, S., Vriens, J., Prenen, J., Benemei, S., De Siena, G., La Marca, G., Andre, E., Preti, D., Avonto, C., & Sadofsky, L. (2012). The 'headache tree' via umbellulone and TRPA1 activates the trigeminovascular system. *Brain*, *135*, 376–390. https://doi.org/10.1093/brain/awr272

Nilius, B., & Voets, T. (2007). Neurophysiology: Channelling cold reception. *Nature*, *448*, 147–148. https://doi.org/10.1038/448147a

Ojewole, J. A. (2005). Antinociceptive, antiinflammatory and antidiabetic effects of *Leonotis leonurus* (L.) R. BR. [Lamiaceae] leaf aqueous extract in mice and rats. *Methods and Findings in Experimental and Clinical Pharmacology*, *27*, 257–264.

Osmanlioglu, H. O., & Naziroglu, M. (2024). Resveratrol modulates diabetes-induced neuropathic pain, apoptosis, and oxidative neurotoxicity in mice through TRPV4 channel inhibition. *Molecular Neurobiology*, *61*, 7269–7286. https://doi.org/10.1007/s12035-024-04311-4

Percie du Sert, N., Hurst, V., Ahluwalia, A., Alam, S., Avey, M. T., Baker, M., Browne, W. J., Clark, A., Cuthill, I. C., Dirnagl, U., Emerson, M., Garner, P., Holgate, S. T., Howells, D. W., Karp, N. A., Lazic, S. E., Lidster, K., MacCallum, C. J., Macleod, M., … Würbel, H. (2020). The ARRIVE guidelines 2.0: Updated guidelines for reporting animal research. *PLoS Biology*, *18*(7), e3000410. https://doi.org/10.1371/journal.pbio.3000410

Proudfoot, C. J., Garry, E. M., Cottrell, D. F., Rosie, R., Anderson, H., Robertson, D. C., Fleetwood-Walker, S. M., & Mitchell, R. (2006). Analgesia mediated by the TRPM8 cold receptor in chronic neuropathic pain. *Current Biology*, *16*, 1591–1605. https://doi.org/10.1016/j.cub.2006.07.061

Rodrigues, P., Ruviaro, N. A., & Trevisan, G. (2022). TRPV4 role in neuropathic pain mechanisms in rodents. *Antioxidants*, *12*, 24. https://doi.org/10.3390/antiox12010024

Sanchez, J. C., Aleman, A., Henao, J. F., Olaya, J. C., & Ehrlich, B. E. (2024). NCS-1 protein regulates TRPA1 channel through the PI3K pathway in breast cancer and neuronal cells. *Journal of Physiology and Biochemistry*, *80*, 451–463. https://doi.org/10.1007/s13105-024-01016-z

Sawada, Y., Hosokawa, H., Matsumura, K., & Kobayashi, S. (2008). Activation of transient receptor potential ankyrin 1 by hydrogen peroxide. *European Journal of Neuroscience*, *27*, 1131–1142. https://doi.org/10.1111/j.1460-9568.2008.06093.x

Shim, H. S., Bae, C., Wang, J., Lee, K. H., Hankerd, K. M., Kim, H. K., Chung, J. M., & la, J. H. (2019). Peripheral and central oxidative stress in chemotherapy-induced neuropathic pain. *Molecular Pain*, *15*, 1744806919840098. https://doi.org/10.1177/1744806919840098

Sousa-Valente, J., Andreou, A. P., Urban, L., & Nagy, I. (2014). Transient receptor potential ion channels in primary sensory neurons as targets for novel analgesics. *British Journal of Pharmacology*, *171*, 2508–2527. https://doi.org/10.1111/bph.12532

Suguro, R., Chen, S., Yang, D., Yang, Z., Miao, L., Wu, W., Zeng, W., Liu, X., & Zhu, Y. Z. (2018). Anti-hypercholesterolemic effects and a good safety profile of SCM-198 in animals: From ApoE knockout mice to rhesus monkeys. *Frontiers in Pharmacology*, *9*, 1468. https://doi.org/10.3389/fphar.2018.01468

Sun, J., Huang, S. H., Zhu, Y. C., Whiteman, M., Wang, M. J., Tan, B. K., & Zhu, Y. Z. (2005). Anti-oxidative stress effects of *Herba leonuri* on ischemic rat hearts. *Life Sciences*, *76*, 3043–3056. https://doi.org/10.1016/j.lfs.2004.11.024

Suzuki, M., Mizuno, A., Kodaira, K., & Imai, M. (2003). Impaired pressure sensation in mice lacking TRPV4. *Journal of Biological Chemistry*, *278*, 22664–22668. https://doi.org/10.1074/jbc.M302561200

Titiz, M., Landini, L., Monteiro, S., de Araujo, D., Marini, M., Seravalli, V., Chieca, M., Pensieri, P., Montini, M., De Siena, G., Pasquini, B., & Vannuccini, S. (2024). Schwann cell C5aR1 co-opts inflammasome NLRP1 to sustain pain in a mouse model of endometriosis. *Nature Communications*, *15*, 10142. https://doi.org/10.1038/s41467-024-54486-6

Trevisan, G., Materazzi, S., Fusi, C., Altomare, A., Aldini, G., Lodovici, M., Patacchini, R., Geppetti, P., & Nassini, R. (2013). Novel therapeutic strategy to prevent chemotherapy-induced persistent sensory neuropathy by TRPA1 blockade. *Cancer Research*, *73*, 3120–3131. https://doi.org/10.1158/0008-5472.CAN-12-4370

Wang, C., Ning, L. P., Wang, Y. H., Zhang, Y., Ding, X. L., Ge, H. Y., Arendt-Nielsen, L., & Yue, S. W. (2011). Nuclear factor-kappa B mediates TRPV4-NO pathway involved in thermal hyperalgesia following chronic compression of the dorsal root ganglion in rats. *Behavioural Brain Research*, *221*, 19–24. https://doi.org/10.1016/j.bbr.2011.02.028

Wang, J., Wang, X. W., Zhang, Y., Yin, C. P., & Yue, S. W. (2015). Ca(2+) influx mediates the TRPV4-NO pathway in neuropathic hyperalgesia following chronic compression of the dorsal root ganglion. *Neuroscience Letters*, *588*, 159–165. https://doi.org/10.1016/j.neulet.2015.01.010

Watanabe, H., Vriens, J., Suh, S. H., Benham, C. D., Droogmans, G., & Nilius, B. (2002). Heat-evoked activation of TRPV4 channels in a HEK293 cell expression system and in native mouse aorta endothelial cells. *Journal of Biological Chemistry*, *277*, 47044–47051. https://doi.org/10.1074/jbc.M208277200

Xu, W., Cui, J., Zhou, F., Bai, M., Deng, R., & Wang, W. (2020). Leonurine protects against dexamethasone-induced cytotoxicity in pancreatic beta-cells via PI3K/Akt signaling pathway. *Biochemical and Biophysical Research Communications*, *529*, 652–658.

Zhang, Y., Guo, W., Wen, Y., Xiong, Q., Liu, H., Wu, J., Zou, Y., & Zhu, Y. (2012). SCM-198 attenuates early atherosclerotic lesions in hypercholesterolemic rabbits via modulation of the inflammatory and oxidative stress pathways. *Atherosclerosis*, *224*, 43–50. https://doi.org/10.1016/j.atherosclerosis.2012.06.066

Zheng, L., Luo, Y., Zhou, D., Liu, H., Zhou, G., Meng, L., Hou, Y., Liu, C., Li, J., & Fu, X. (2023). Leonurine improves bovine oocyte maturation and subsequent embryonic development by reducing oxidative stress and improving mitochondrial function. *Theriogenology*, *199*, 11–18. https://doi.org/10.1016/j.theriogenology.2023.01.010

Zhu, Y. Z., Wu, W., Zhu, Q., & Liu, X. (2018). Discovery of Leonuri and therapeutical applications: From bench to bedside. *Pharmacology & Therapeutics*, *188*, 26–35. https://doi.org/10.1016/j.pharmthera.2018.01.006

Zimmermann, M. (1983). Ethical guidelines for investigations of experimental pain in conscious animals. *Pain*, *16*, 109–110. https://doi.org/10.1016/0304-3959(83)90201-4

Zurborg, S., Piszczek, A., Martínez, C., Hublitz, P., Al Banchaabouchi, M., Moreira, P., Perlas, E., & Heppenstall, P. A. (2011). Generation and characterization of an Advillin-Cre driver mouse line. *Molecular Pain*, *7*, 66. https://doi.org/10.1186/1744-8069-7-66

SUPPORTING INFORMATION

Additional supporting information can be found online in the Supporting Information section at the end of this article.

How to cite this article: Marini, M., Landini, L., Coppi, E., Tesi, M., Bellantoni, E., Chieca, M., Croce, E. B., Bonacchi, L., Brancolini, G., Bruschi, P., de Araújo, D. S. M., De Siena, G., Dimitrova, A., Mastricci, A., Rocha Mendonça, H., Scuffi, I., Venturini, M., Dos Santos Heringer, L., Vaiano, F., … De Logu, F. (2025). Anti-nociceptive action of leonurine through TRPA1 and TRPV4 channels modulation. *British Journal of Pharmacology*, *182*(22), 5469–5488. https://doi.org/10.1111/bph.70135